ATMOSPHERIC REFRACTION EFFECTS ON BASELINE ERROR IN SATELLITE LASER RANGING SYSTEMS

by

K. E. Im
C. S. Gardner

RRL Publication No. 519

Technical Report
September 1982

Supported by
Contract No. NASA NSG-5049

NATIONAL AERONAUTICS & SPACE ADMINISTRATION
Goddard Space Flight Center
Greenbelt, Maryland 20771

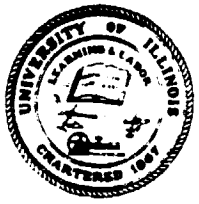

RADIO RESEARCH LABORATORY
DEPARTMENT OF ELECTRICAL ENGINEERING
COLLEGE OF ENGINEERING
UNIVERSITY OF ILLINOIS
URBANA, ILLINOIS 61801

ATMOSPHERIC REFRACTION EFFECTS ON BASELINE ERROR IN SATELLITE LASER RANGING SYSTEMS

by

K. E. Im
C. S. Gardner

RRL Publication No. 519

Technical Report
September 1982

Supported by
Contract No. NASA NSG-5049

NATIONAL AERONAUTICS & SPACE ADMINISTRATION
Goddard Space Flight Center
Greenbelt, Maryland 20771

RADIO RESEARCH LABORATORY
DEPARTMENT OF ELECTRICAL ENGINEERING
COLLEGE OF ENGINEERING
UNIVERSITY OF ILLINOIS
URBANA, ILLINOIS 61801

TABLE OF CONTENTS

II to III

LIST OF FIGURES

Figure | Page

1. INTRODUCTION

Satellite laser ranging systems are currently being used to accurately measure the baseline distances between widely spearated points on the earth's surface [1]. The technique involves measuring the distances between the ground stations and retroreflector equipped satellites [2]. Typically, hundreds of range measurements are obtained during a single satellite pass over a ground station. Measurements from several passes are used to determine the satellite orbit and the coordinates of the ground sites. Major error sources include instrumentation noise, orbit modeling errors and atmospheric refraction. The effects of these errors on baseline accuracy is a complicated function of the geometry of the satellite orbits and ground station locations. In this paper we are primarily concerned with the effects of atmospheric refraction. Unfortunately, because of the mathematical complexities involved in exact analyses of baseline errors, it is not easy to isolate the atmospheric refraction effects. However, by making certain simplifying assumptions about the ranging system geometry, relatively simple expressions can be derived which relate the baseline errors directly to the refraction errors. The results indicate that even in the absence of other errors, the baseline error for intercontinental baselines can be more than an order of magnitude larger than the refraction error.

2. BASELINE ERROR ANALYSIS

The general nonlinear regression model of n measurements [3] is given by

$$\underline{y} = \underline{f}(\underline{x},\underline{s}) + \underline{\varepsilon} \qquad (1)$$

where $\underline{x}$ contains epoch values of the desired parameters to be estimated, $\underline{s}$ contains epoch values of the unadjusted parameters which are assumed to be known constants in solving the regression equations, and $\underline{\varepsilon}$ is the zero mean measurement noise vector. It is assumed that the elements of $\underline{\varepsilon}$ are statistically independent, and the partitioning of parameters into $\underline{x}$ and $\underline{s}$ is arbitrary.

When this regression equation is used to model the distance measurements between a ground station and the satellite, $\underline{y}$ is a vector representing the range measurements between a ground station and the satellite, $\underline{x}$ is a vector representing the epoch values of the ground station coordinates, and $\underline{s}$ is a vector representing the epoch values of the error sources' parameters such as the orbit modeling errors and the atmospheric refraction errors. The vector function $\underline{f}(\underline{x},\underline{s})$ in Equation (1) can be defined as

$$\underline{f}(\underline{x},\underline{s}) = \underline{D} + \underline{AR} \qquad (2)$$

where $\underline{D}$ is a vector representing the actual geometric distances between the ground stations and the satellite, and $\underline{AR}$ is a vector representing the atmospheric refraction.

The total error covariance matrix associated with the station coordinates for this model is given by [3]

$$E[(\Delta\underline{x})(\Delta\underline{x})^T] = (\underline{A}^T\underline{W}\underline{A} + \underline{P}_a^{-1})^{-1} + (\underline{A}^T\underline{W}\underline{A} + \underline{P}_a^{-1})^{-1}\ (\underline{A}^T\underline{W}\underline{B})\ \underline{V}_s\ (\underline{B}^T\underline{W}\underline{A}) \cdot (\underline{A}^T\underline{W}\underline{A} + \underline{P}_a^{-1})^{-1} \quad (3)$$

where

$$A = \left.\frac{\partial \underline{f}(\underline{x},\underline{s})}{\partial \underline{x}}\right|_{\substack{\underline{x} = \underline{x}_N \\ \underline{s} = \underline{s}_N}}, \quad (4)$$

$$B = \left.\frac{\partial \underline{f}(\underline{x},\underline{s})}{\partial \underline{s}}\right|_{\substack{\underline{x} = \underline{x}_N \\ \underline{s} = \underline{s}_N}}, \quad (5)$$

$\underline{P}_a$ is the covariance matrix for the *a priori* estimate of the station coordinates $\underline{x}$, $\underline{W}$ is the inverse of the measurement noise covariance matrix, $\underline{V}_s$ is the covariance matrix associated with the unadjusted parameter $\underline{s}$, and $\underline{x}_N$ and $\underline{s}_N$ are the nominal values for $\underline{x}$ and $\underline{s}$, respectively.

The elements of the matrix $\underline{W}$ are directly proportional to the total number of range measurements. So in satellite laser ranging where a large number of range measurements is obtained, the $\underline{P}_a^{-1}$ matarix in Equation (3) can be neglected when it is compared to the $\underline{A}^T\underline{W}\underline{A}$ matrix. That is, the a priori estimate of $\underline{x}$ is not as critical in determining the error covariance matrix when a large number of range measurements is gathered. Because of this and the fact that the $(\underline{A}^T\underline{W}\underline{A})^{-1}$ matrix is small, Equation (3) can be simplified to

$$E[(\Delta\underline{x})(\Delta\underline{x})^T] = (\underline{A}^T\underline{W}\underline{A})^{-1}\,(\underline{A}^T\underline{W}\underline{B})\,\underline{V}_s\,(\underline{B}^T\underline{W}\underline{A})(\underline{A}^T\underline{W}\underline{A})^{-1} \tag{6}$$

In Cartesian coordinates, the baseline distance between two points can be expressed as

$$B_L = [(x_1 - x_2)^2 + (y_1 - y_2)^2 + (z_1 - z_2)^2]^{1/2} \tag{7}$$

where (x_1, y_1, z_1) and (x_2, y_2, z_2) are the coordinates of the two points of interest. By letting Δx_m, Δy_m, Δz_m denote the coordinate measurement errors associated with the mth station (m = 1,2), the baseline error can be expressed mathematically by expanding Equation (7) in a Taylor series about the current nominal parameter $\underline{x}_N$,

$$B_L \approx \left.\frac{\partial B_L}{\partial x_1}\right|_{\underline{x}=\underline{x}_N} \Delta x_1 + \left.\frac{\partial B_L}{\partial x_2}\right|_{\underline{x}=\underline{x}_N} \Delta x_2 + \left.\frac{\partial B_L}{\partial y_1}\right|_{\underline{x}=\underline{x}_N} \Delta y_1$$

$$+ \left.\frac{\partial B_L}{\partial y_2}\right|_{\underline{x}=\underline{x}_N} \Delta y_2 + \left.\frac{\partial B_L}{\partial z_1}\right|_{\underline{x}=\underline{x}_N} \Delta z_1 + \left.\frac{\partial B_L}{\partial z_2}\right|_{\underline{x}=\underline{x}_N} \Delta z_2 \ . \tag{8}$$

It can be seen from Equation (8) that the mean square baseline error consists of the variances and the covariances of the various coordinate errors. By explicitly evaluating Equation (6) and using the results with Equation (8), the baseline error can be determined.

3. RANGING GEOMETRY

As mentioned in Section 1, the major error sources for the baseline determination include the orbit modeling errors and the atmospheric refraction errors. In this analysis, we want to reduce all other error sources to negligible levels in order to estimate the ultimate effect of refraction on the baseline errors. By doing so, we are assuming that the orbit modeling errors are negligible. This is a reasonable assumption because, in practice, several days' worth of data from many stations are used to determine the best fit satellite orbit [4]. The station coordinates are then determined using this best fit orbit. In this section, a particular ranging geometry for the best fit satellite orbit is defined and used to calculate the baseline error.

The geometry of the two ground stations and the two satellite paths is illustrated in Figure 1. Notice that two satellite passes are required to solve for the ground station coordinates. The satellite ground tracks are parallel to each other, and the satellite altitudes (h) are constant and equal for the two passes. This corresponds roughly to the geometry for a polar, circular orbit satellite. Furthermore, high altitude orbits are assumed so that a flat-earth model can be employed in the analysis to simplify the mathematics. It should be noted that the results otained by using the flat-earth model will not differ substantially from those obtained by using the spherical-earth model.

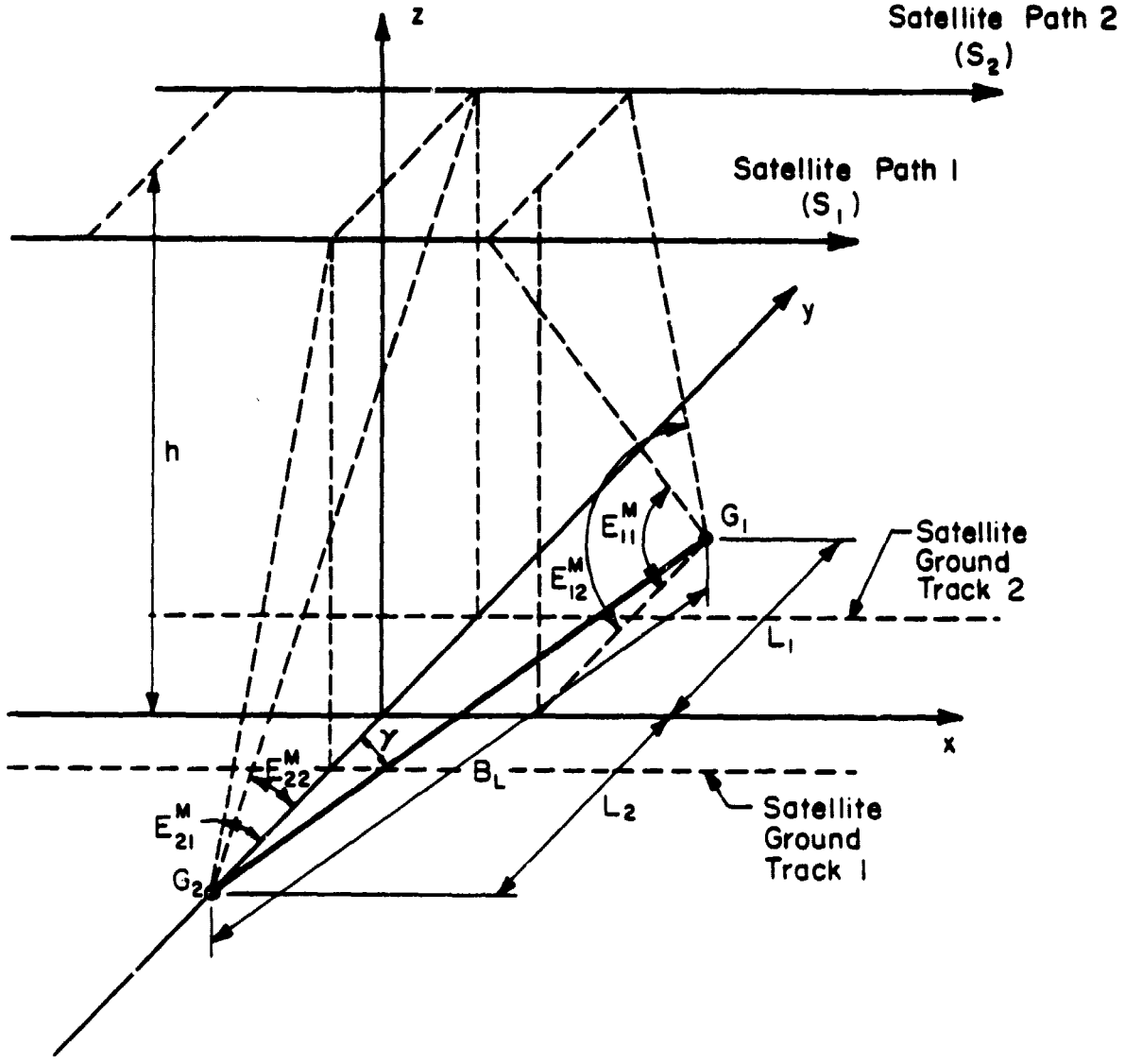

Figure 1. Geometry of the two-ground-station, two-satellite-pass ranging system.

For simplicity, the satellite orbits, S_1 and S_2, are assumed to be in the x-direction. The nominal coordinates of the ground station 1 (G_1) are $((L_1 + L_2) \tan \gamma, L_1, 0)$ and the nominal coordinates of the ground station 2 (G_2) are $(0,-L_2,0)$. The baseline between the two stations and the y-axis intersect at an angle γ. The maximum elevation angle associated with the mth ground station and the nth satellite pass is denoted by

$$E^M_{mn} \qquad m = 1,2, \quad n = 1,2 \ .$$

For this particular geometry ,

$$\left.\frac{\partial B_L}{\partial x_m}\right|_{\underline{x} = \underline{x}_N} \qquad \Delta x_m = (-1)^{m+1} \Delta x_m \sin \gamma \qquad m = 1,2 \ , \tag{9}$$

$$\left.\frac{\partial B_L}{\partial y_m}\right|_{\underline{x} = \underline{x}_N} \qquad \Delta y_m = (-1)^{m+1} \Delta y_m \cos \gamma \qquad m = 1,2 \ , \tag{10}$$

and

$$\left.\frac{\partial B_L}{\partial z_m}\right|_{\underline{x} = \underline{x}_N} \qquad \Delta z_m = 0 \qquad m = 1,2 \ . \tag{11}$$

By substituting Equations (9) through (11) into Equation (8), we have

$$\Delta B_L = \sin \gamma \, (\Delta x_1 - \Delta x_2) + \cos \gamma \, (\Delta y_1 - \Delta y_2) \ . \tag{12}$$

The mean square baseline error is, therefore, given by

$$\langle \Delta B_L^2 \rangle = \sin^2 \gamma \left[\sigma_{x_1}^2 - 2\,\mathrm{cov}(x_1,x_2) + \sigma_{x_2}^2\right]$$

$$+ \cos^2 \gamma \left[\sigma_{y_1}^2 - 2\,\mathrm{cov}(y_1,y_2) + \sigma_{y_2}^2\right]$$

$$+ 2 \sin \gamma \cos \gamma \left[\mathrm{cov}(x_1,y_1) - \mathrm{cov}(x_1,y_2) - \mathrm{cov}(y_1,x_2)\right.$$

$$\left. + \mathrm{cov}(x_2,y_2)\right] \quad . \qquad (13)$$

4. BASELINE ERROR FOR THE SPHERICALLY SYMMETRIC ATMOSPHERE

The various matrices mentioned in Section 2 will be formulated here for the ranging geometry of Section 3. For this ranging model, the orbit modeling errors have been assumed to be negligible and the dominant errors associated with the range measurements are the atmospheric refraction errors and the instrumentation errors.

Normally, the range measurements are taken when the elevation angles are above certain threshold angles E^0_{mn} and they are taken uniformly in time during the satellite pass (refer to Figure 2). Thus, we can denote the position of the satellite during the jth measurement by its Cartesian coordinates as

$$(x_{Sj}, y_{Sj}, z_{Sj}) = \begin{cases} \text{position of satellite on orbit } S_1 \text{ during the jth measurement for station } G_1 & \text{if } 1 \leq j \leq k \\ \text{position of satellite on orbit } S_2 \text{ during the jth measurement for station } G_1 & \text{if } k+1 \leq j \leq 2k \\ \text{position of satellite on orbit } S_1 \text{ during the jth measurement for station } G_2 & \text{if } 2k+1 \leq j \leq 3k \\ \text{position of satellite on orbit } S_2 \text{ during the jth measurement for station } G_2 & \text{if } 3k+1 \leq j \leq 4k. \end{cases}$$

It should be noted that the threshold elevation angles associated with each ground station and each satellite pass are different, but they are usually related to one another for a particular geometry. Further discussion on their relationship is given later in this section.

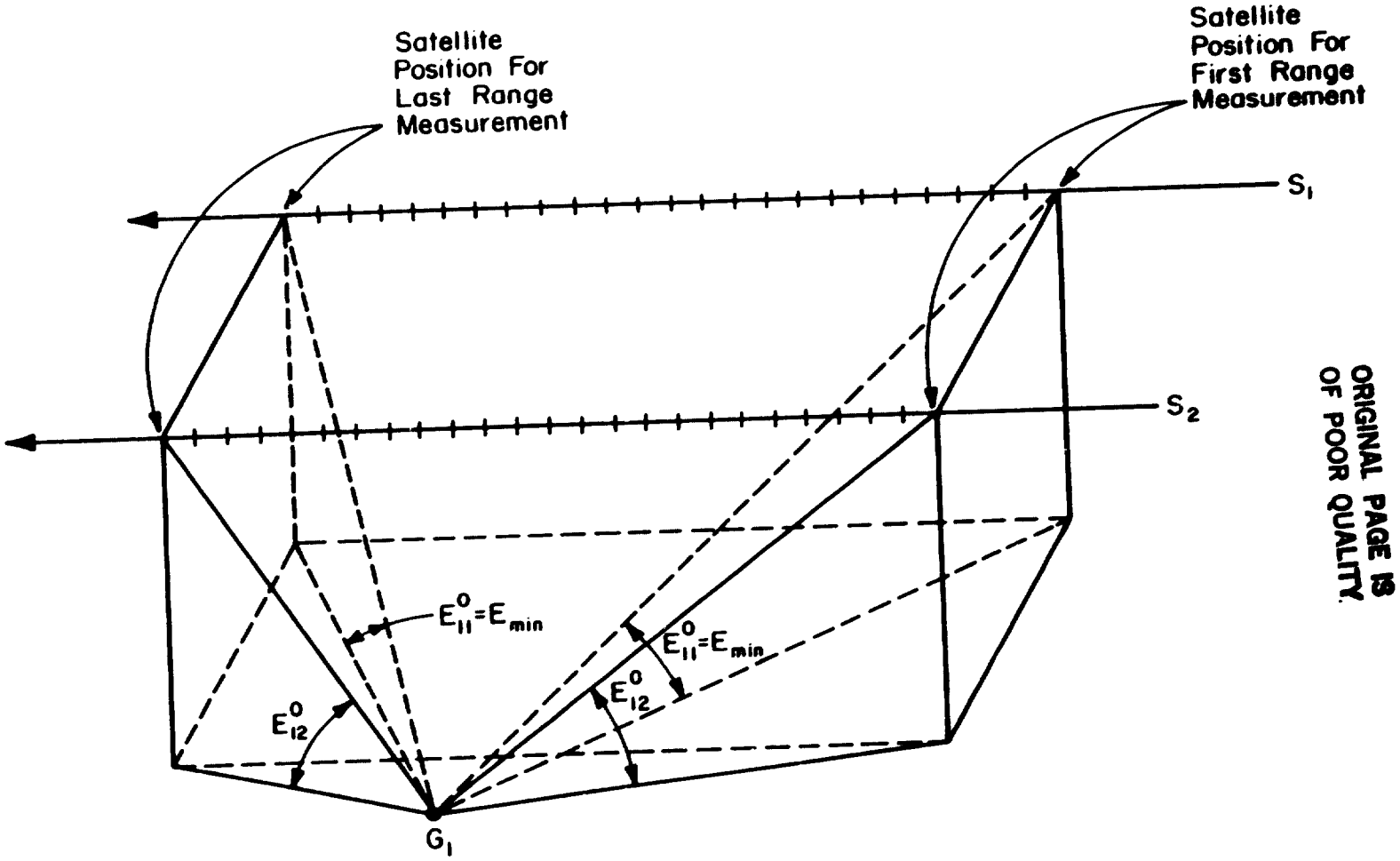

Figure 2. Threshold elevation angles associated with ground station 1 and the two satellite paths.

If G_1 and G_2 are located at (x_1,y_1,z_1) and (x_2,y_2,z_2), respectively, then the geometric distances between the ground stations and the satellite at various points along the satellite orbits can be written as

$$d_j = \begin{cases} [(x_{Sj}-x_1)^2+(y_{Sj}-y_1)^2+(h-z_1)^2]^{1/2} & \text{geometric distances between } G_1 \text{ and satellite along } S_1 \text{ if } 1 \le j \le k \\ [(x_{Sj}-x_1)^2+(y_{Sj}-y_1)^2+(h-z_1)^2]^{1/2} & \text{geometric distance between } G_1 \text{ and satellite along } S_2 \text{ if } k+1 \le j \le 2k \\ [(x_{Sj}-x_2)^2+(y_{Sj}-y_2)^2+(h-z_2)^2]^{1/2} & \text{geometric distance between } G_2 \text{ and satellite along } S_1 \text{ if } 2k+1 \le j \le 3k \\ [(x_{Sj}-x_2)^2+(y_{Sj}-y_2)^2+(h-z_2)^2]^{1/2} & \text{geometric distance between } G_2 \text{ and satellite along } S_2 \text{ if } 3k+1 \le j \le 4k, \end{cases} \tag{14}$$

and the column vector $\underline{D}$ of Equation (2) can be expressed as

$$\underline{D} = [d_1,\ldots,d_{4k}]^T \quad . \tag{15}$$

For a spherically symmetric atmosphere, the effects of horizontal refractivity gradients [5] are negligible, and the atmospheric refraction associated with the jth range measurement is given by [6]

$$AR_j = \frac{\beta_j}{\sin E_j} \qquad j = 1,\ldots,4k \tag{16}$$

where E_j is the elevation angle associated with the ground station and the satellite at the jth measurement, and β_j is the spherical correction coefficient associated with the jth measurement. β_j is a function of surface pressure, temperature and the water vapor pressure at the ranging sites during the satellite passes [6]. By referring to the ranging geometry of Figure 2, Equation (16) can also be expressed as

$$AR_j = \frac{\beta_j d_j}{h} \qquad j = 1,\ldots,4k \quad . \tag{17}$$

By using the results of Equation (17), the column vector $\underline{AR}$ of Equation (2) can now be expressed explicitly as

$$\underline{AR} = \left[\frac{\beta_1 d_1}{h}, \ldots, \frac{\beta_{4k} d_{4k}}{h}\right]^T \quad . \tag{18}$$

By substituting Equations (15) and (18) into Equation (2), the range distance vector $\underline{f}(\underline{x},\underline{s})$ in the spherically symmetric atmosphere can be written as

$$\underline{f}(\underline{x},\underline{s}) = \left[\left(1 + \frac{\beta_1}{h}\right) d_1, \ldots, \left(1 + \frac{\beta_{4k}}{h}\right) d_{4k}\right]^T \quad . \tag{19}$$

The spherical correction coefficients vary from measurement to measurement, depending on the instantaneous weather conditions at the ranging sites and along the optical path. So the unadjusted parameter vector $\underline{s}$ should be expressed as

$$\underline{s} = [\beta_1, \ldots, \beta_{4k}]^T \quad . \tag{20}$$

Since the time period for each satellite pass is usually short, substantial changes in the weather conditions at the ground stations are not expected. Typically, meteorological data is acquired once during each satellite pass and used to calculate β to correct the ranging data collected during that pass. Therefore, we assume that the value of β that is used to correct the measurements for a ground station remains constant on the same satellite pass.

The ground stations are usually widely separated so that the surface pressure, temperature and the water vapor pressure at these stations may be completely different from and independent of each other. As a result, the meteorological data, and hence the β's, associated with different grouud stations, are assumed to be independent. Consequently, the errors in calculating these β's ($\Delta\beta$'s) at the two ground stations are assumed to be uncorrelated. Notice that these errors arise from inaccuracies in the formulas used to predict β from meteorological parameters and from errors in the meteorological measurements.

Due to the assumptions of constant β for the same satellite pass and different β's between ground stations, Equation (20) can be simplified as

$$\underline{s} = [\beta_{11} \ \beta_{12} \ \beta_{21} \ \beta_{22}]^T \tag{21}$$

where β_{mn} is the estimated spherical correction coefficient associated with the mth ground station during the nth pass.

Because the range measurements in the two passes are taken at different times, the correlation of $\Delta\beta$ between passes can either be high or low, depending on the extent of the weather changes during the two passes. When the temporal separation between passes is short or when the weather conditions at the ground stations are fairly constant during the two passes, we would expect to see a very high correlation betwen the values of β for the two passes. Therefore, the errors in β, i.e., $\Delta\beta$, would be expected to be correlated for the two passes. Conversely, if the time separating the two passes is long or if weather conditions changed substantially, a partial or a relatively low correlation between $\Delta\beta$ during the two

passes would be expected. In Section 4.1, a general expression for the baseline error in the spherically symmetric atmosphere is derived.

4.1 General Expression for the Baseline Error

Before we can derive a general expression for the baseline error, the various matrices of Equation (3) must be expressed explicitly in terms of the relative positions of the satellite and the ground stations according to the prescribed geometry.

By replacing the general β's of Equation (20) with the station-varying and path-varying β_{mn}'s, we obtain a simplified expression for the range distance vector $\underline{f}(\underline{x},\underline{s})$ as

$$\underline{f}(\underline{x},\underline{s}) = \left[\left(1+\frac{\beta_{11}}{h}\right)d_1,\ldots,\left(1+\frac{\beta_{11}}{h}\right)d_k \vdots \left(1+\frac{\beta_{12}}{h}\right)d_{k+1},\ldots,\left(1+\frac{\beta_{12}}{h}\right)d_{2k} \vdots \left(1+\frac{\beta_{21}}{h}\right)d_{2k+1},\ldots,\left(1+\frac{\beta_{21}}{h}\right)d_{3k} \vdots \left(1+\frac{\beta_{22}}{h}\right)d_{3k+1},\ldots,\left(1+\frac{\beta_{22}}{h}\right)d_{4k}\right]^T \tag{22}$$

where d_j is a function of both the station coordinates and the current satellite positions, and

$$\underline{x} = [x_1\ y_1\ z_1\ x_2\ y_2\ z_2]^T \tag{23}$$

is the ground station coordinate vector.

The partial derivative of $\underline{f}(\underline{x},\underline{s})$ with respect to $\underline{x}$ can be calculated by differentiating each vector component of Equation (22) with respect to each vector component of Equation (23). For instance, differentiating the first component of Equation (22) with respect to the x-coordinate of the ground station 1 yields

$$\frac{\partial[(1 + \frac{\beta_{11}}{h})\, d_1]}{\partial x_1} = -\left(1 + \frac{\beta_{11}}{h}\right)\frac{x_1}{d_1} \quad . \tag{24}$$

Notice that the resulting partial derivative $\frac{\partial \underline{f}}{\partial \underline{x}}$ is a 4k by 6 matrix. After evaluating this matrix at the nominal station coordinates of $((L_1 + L_2)\tan\gamma,\ L_1,\ 0)$ and $(0,-L_2,0)$(refer to Figure 1), the $\underline{A}$ matrix of Equation (4) can be expressed explicitly as

$$\underline{A} = -\begin{bmatrix} \left(1+\frac{\beta_{11}}{h}\right)\frac{x_1}{d_1} & \left(1+\frac{\beta_{11}}{h}\right)\frac{(y_1-L_1)}{d_1} & \left(1+\frac{\beta_{11}}{h}\right)\frac{h}{d_1} & & & \\ \vdots & \vdots & \vdots & & \bigcirc & \\ \left(1+\frac{\beta_{12}}{h}\right)\frac{x_{2k}}{d_{2k}} & \left(1+\frac{\beta_{12}}{h}\right)\frac{(y_{2k}-L_1)}{d_{2k}} & \left(1+\frac{\beta_{12}}{h}\right)\frac{h}{d_{2k}} & & & \\ & & & \left(1+\frac{\beta_{21}}{h}\right)\frac{x_{2k+1}}{d_{2k+1}} & \left(1+\frac{\beta_{21}}{h}\right)\frac{(y_{2k+1}+L_2)}{d_{2k+1}} & \left(1+\frac{\beta_{21}}{h}\right)\frac{h}{d_{2k+1}} \\ & \bigcirc & & \vdots & \vdots & \vdots \\ & & & \left(1+\frac{\beta_{22}}{h}\right)\frac{x_{4k}}{d_{4k}} & \left(1+\frac{\beta_{22}}{h}\right)\frac{(y_{4k}+L_2)}{d_{4k}} & \left(1+\frac{\beta_{22}}{h}\right)\frac{h}{d_{4k}} \end{bmatrix}. \tag{25}$$

The partial derivative of $\underline{f}(\underline{x},\underline{s})$ with respect to $\underline{s}$ can be calculated by differentiating each vector component of Equation (22) with respect to each vector component of Equation (21). The resulting matrix is a 4k by 4 matrix. After evaluating this matrix at the nominal station coordinates, the $\underline{B}$ matrix of Equation (5) can be expressed explicitly as

$$\underline{B} = \begin{bmatrix} \frac{d_1}{h} & \cdots & \frac{d_k}{h} & 0 & \cdots & 0 \\ 0 & \cdots & 0 & \frac{d_{k+1}}{h} & \cdots & \frac{d_{2k}}{h} & 0 & \cdots & 0 \\ 0 & \cdots & 0 & \frac{d_{2k+1}}{h} & \cdots & \frac{d_{3k}}{h} & 0 & \cdots & 0 \\ 0 & \cdots & 0 & \frac{d_{3k+1}}{h} & \cdots & \frac{d_{4k}}{h} \end{bmatrix}^T . \qquad (26)$$

In order to derive an explicit expression for the $\underline{W}$ matrix, we have to investigate the statistics of the measurement noise in the satellite laser ranging system. It has been shown that the photoelectron distribution from a single-mode laser follows Poisson [7]. Recently, the MMSE and ML estimator noise variances for the laser ranging receiver have also been derived [8]. In particular, if the received optical pulse shape closely approximates a Gaussian pulse shape, and if no background noise is present in the system, the ML estimator noise variance for each range measurement is given by [8]

$$\sigma^2 = \frac{b^2}{4\pi^2 Q} \qquad (27)$$

where b is the full width of the optical pulse measured at half maximum (FWHM), and Q is the average number of photoelectrons per pulse.

The average number of photoelectrons in a received pulse is directly proportional to the received pulse strength, which in turn is inversely proportional to the geometric distance between the ground station and the satellite. In a vacuum, this signal pulse strength decreases inversely

with the square of the distance. In the earth's atmosphere where absorption and scattering increase with pathlength, the signal pulse strength may decrease even more quickly.

In the satellite laser ranging system, both the laser transmitter and the receiver are located at the ground stations, and retroreflectors are installed on the satellite. The transmitter sends out pulses at a constant repetition rate during the ranging period. These pulses are then reflected back from the retroreflector-equipped satellite and are detected by the receiver. The time of flight of the laser pulse is measured through the range counter, which is then multiplied by the velocity of light in the atmosphere to give the range to the satellite [2], [9].

In this configuration, the optical pulses travel twice the station-to-satellite distance. So the received pulse strength, and therefore the number of photoelectrons per pulse, is inversely proportional to the fourth power of the distance, and the measurement noise variance can be expressed as

$$\sigma_j^2 = \sigma_\epsilon^2 d_j^4 \qquad j = 1,\ldots,4k \tag{28}$$

where σ_ϵ^2 is called the measurement noise variance factor. By using the result of Equation (28), we can obtain the inverse of the measurement noise covariance matrix as

$$\underline{W} = \frac{1}{\sigma_\epsilon^2} \operatorname{diag}\left[\frac{1}{d_1^4} \cdots \frac{1}{d_{4k}^4}\right] . \tag{29}$$

By the previous assumptions that the errors in β's ($\Delta\beta$) between stations are uncorrelated and that the degree of β-error correlation between

passes depends upon differences in the stations' weather conditions during the two passes, the covariance matrix associated with the vector $\underline{s}$ can be expressed as

$$\underline{V}_s = \sigma_\beta^2 \begin{bmatrix} 1 & \rho_1 & & \\ \rho_1 & 1 & & \\ & & 1 & \rho_2 \\ & & \rho_2 & 1 \end{bmatrix} \tag{30}$$

where σ_β^2 is the variance of β, and ρ_m, $m = 1,2$ is the β-error correlation coefficient associated with the measurements acquired for the mth station during the two passes.

By substituting Equations (25), (26), (29) and (30) into Equation (6) and carrying out the appropriate matrix operations, the error covariance matrix associated with the station coordinates can be obtained as

$$E[(\Delta\underline{x})(\Delta\underline{x})^T] = \begin{bmatrix} 0 & 0 & 0 & 0 & 0 & 0 \\ 0 & \sigma_{y_1}^2 & \text{cov}(y_1,z_1) & 0 & 0 & 0 \\ 0 & \text{cov}(y_1,z_1) & \sigma_{z_1}^2 & 0 & 0 & 0 \\ 0 & 0 & 0 & 0 & 0 & 0 \\ 0 & 0 & 0 & 0 & \sigma_{y_2}^2 & \text{cov}(y_2,z_2) \\ 0 & 0 & 0 & 0 & \text{cov}(y_2,z_2) & \sigma_{z_2}^2 \end{bmatrix} \tag{31}$$

where

$$\sigma_{y_1}^2 = \frac{\sigma_\beta^2 \sin^2 E_{11}^M \sin^2 E_{12}^M}{\sin^2(E_{11}^M - E_{12}^M)} \left[\frac{C_{11}^2}{\sin^4 E_{11}^M} - \frac{2\rho_1 C_{11} C_{12}}{\sin^2 E_{11}^M \sin^2 E_{12}^M} + \frac{C_{12}^2}{\sin^4 E_{12}^M} \right], \tag{32}$$

$$\mathrm{cov}(y_1,z_1) = \frac{\sigma_\beta^2 \sin^2 E_{11}^M \sin^2 E_{12}^M}{\sin^2(E_{11}^M - E_{12}^M)}\left[\frac{C_{11}^2}{\sin^4 E_{11}^M \sin^2 E_{12}^M} - \frac{\rho_1 C_{11} C_{12}}{\sin^2 E_{11}^M \sin^2 E_{12}^M}\right.$$

$$\left.\cdot(\cot E_{11}^M + \cot E_{12}^M) + \frac{C_{12}^2}{\sin^4 E_{12}^M \tan E_{11}^M}\right] \quad , \qquad (33)$$

$$\sigma_{z_1}^2 = \frac{\sigma_\beta^2 \sin^2 E_{11}^M \sin^2 E_{12}^M}{\sin^2(E_{11}^M - E_{12}^M)}\left[\frac{C_{11}^2}{\sin^4 E_{11}^M \tan^2 E_{12}^M}\right.$$

$$\left. - \frac{2\rho_1 C_{11} C_{12}}{\sin^2 E_{11}^M \sin^2 E_{12}^M \tan E_{11}^M \tan E_{12}^M} + \frac{C_{12}^2}{\sin^4 E_{12}^M \tan^2 E_{11}^M}\right] \quad , \qquad (34)$$

$$\sigma_{y_2}^2 = \frac{\sigma_\beta^2 \sin^2 E_{21}^M \sin^2 E_{22}^M}{\sin^2(E_{21}^M - E_{22}^M)}\left[\frac{C_{21}^2}{\sin^4 E_{21}^M} - \frac{2\rho_2 C_{21} C_{22}}{\sin^2 E_{21}^M \sin^2 E_{22}^M} + \frac{C_{22}^2}{\sin^4 E_{22}^M}\right] , \qquad (35)$$

$$\operatorname{cov}(y_2,z_2) = \frac{\sigma_\beta^2 \sin^2 E_{21}^M \sin^2 E_{22}^M}{\sin^2(E_{21}^M - E_{22}^M)} \left[\frac{C_{21}^2}{\sin^4 E_{21}^M \tan E_{22}^M} - \frac{\rho_2 C_{21} C_{22}}{\sin^2 E_{21}^M \sin^2 E_{22}^M} \right.$$

$$\left. \cdot(\cot E_{21}^M + \cot E_{22}^M) + \frac{C_{22}^2}{\sin^4 E_{22}^M \tan E_{21}^M} \right] , \qquad (36)$$

$$\sigma_{z_2}^2 = \frac{\sigma_\beta^2 \sin^2 E_{21}^M \sin^2 E_{22}^M}{\sin^2(E_{21}^M - E_{22}^M)} \left[\frac{C_{21}^2}{\sin^4 E_{21}^M \tan^2 E_{22}^M} \right.$$

$$\left. - \frac{2\rho_2 C_{21} C_{22}}{\sin^2 E_{21}^M \sin^2 E_{22}^M \tan E_{21}^M \tan E_{22}^M} + \frac{C_{22}^2}{\sin^4 E_{22}^M \tan^2 E_{21}^M} \right] , \qquad (37)$$

$$C_{mn} = \frac{\frac{1}{4} \sin 2\phi_{mn} + \frac{1}{2} \phi_{mn}}{\frac{1}{32} \sin 4\phi_{mn} + \frac{1}{4} \sin 2\phi_{mn} + \frac{3}{8} \phi_{mn}} , \quad m = 1,2, \quad n = 1,2 \qquad (38)$$

and

$$\phi_{mn} = \cos^{-1}\left(\frac{\sin E_{mn}^0}{\sin E_{mn}^M} \right) , \quad m = 1,2, \quad n = 1,2 . \qquad (39)$$

Equation (38) is plotted versus ϕ_{mn} in Figure 3. This figure shows that the effective bounds for C_{mn} are

$$1 < C_{mn} < 4/3 \qquad \text{for} \quad 0 < \phi_{mn} < \frac{\pi}{2} \text{ radians} .$$

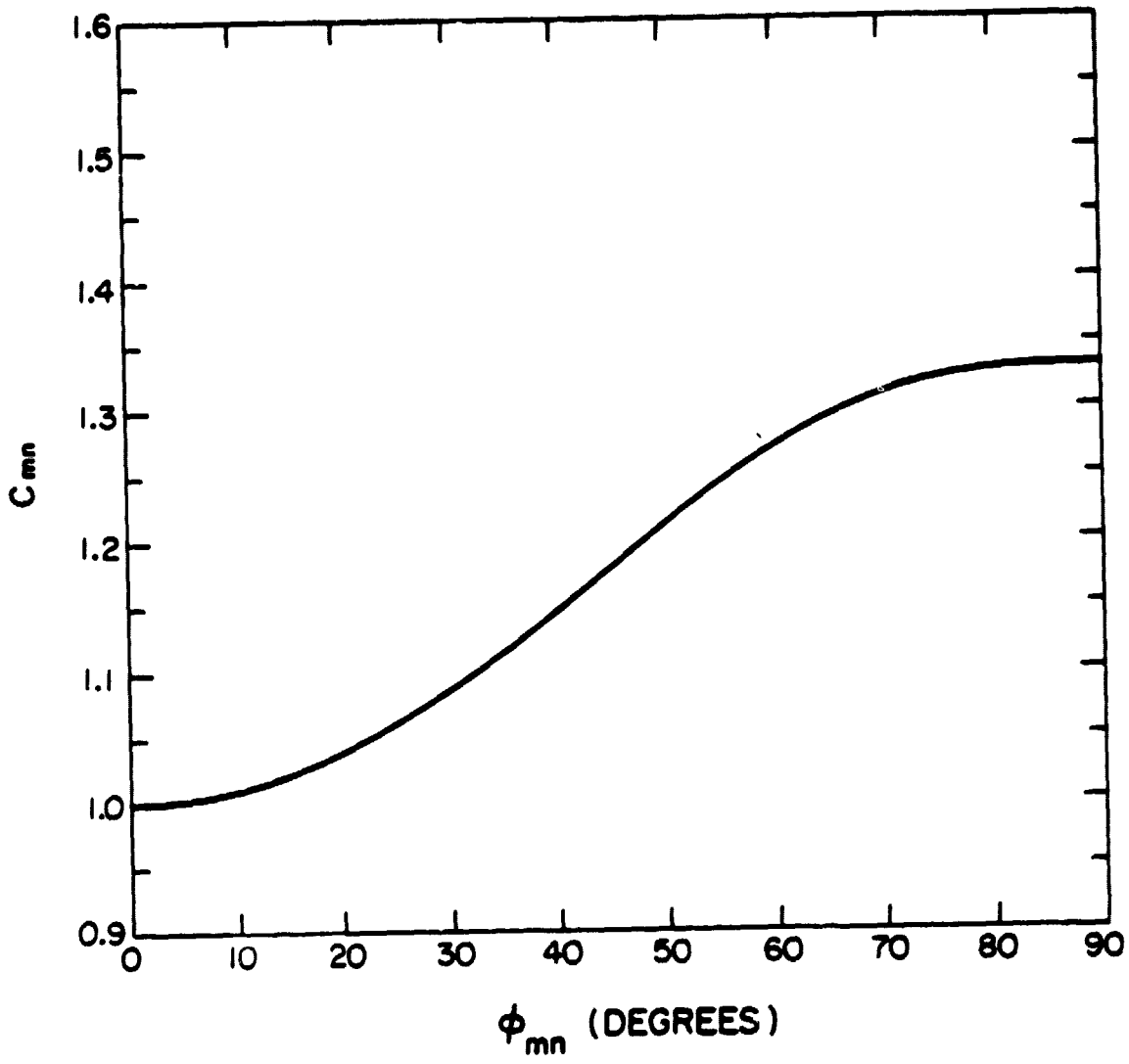

Figure 3. The effective bounds for C_{mn}.

This small range of C_{mn} indicates that C_{mn} is very insensitive to changes of various parameters.

Equation (31) indicates that the position errors between the two ground stations are uncorrelated. This is to be expected since the meteorological data errors and measurement errors are uncorrelated between the widely separated stations. Furthermore, because of symmetry, the x-coordinate errors made on the two passes offseting each other, and the net x-coordinate range error (the x-axis is parallel to the satellite paths) for each station is zero. Therefore, $\sigma^2_{x_1}$, $\mathrm{cov}(x_1,y_1)$, $\mathrm{cov}(x_1,z_1)$, $\sigma^2_{x_2}$, $\mathrm{cov}(x_2,y_2)$ and $\mathrm{cov}(x_2,z_2)$ all have zero entries.

By substituting Equations (31), (32), and (35) into Equation (13), an explicit expression for $\langle \Delta B_L^2 \rangle$ for the satellite laser ranging system in the spherically symmetric atmosphere can be obtained

$$\langle \Delta B_L^2 \rangle = \sigma_\beta^2 \cos^2\gamma \left\{ \frac{\sin^2 E_{11}^M \sin^2 E_{12}^M}{\sin^2(E_{11}^M - E_{12}^M)} \left[\frac{C_{11}^2}{\sin^4 E_{11}^M} - \frac{2\rho_1 C_{11} C_{12}}{\sin^2 E_{11}^M \sin^2 E_{12}^M} + \frac{C_{12}^2}{\sin^4 E_{12}^M} \right] + \frac{\sin^2 E_{21}^M \sin^2 E_{22}^M}{\sin^2(E_{21}^M - E_{22}^M)} \left[\frac{C_{21}^2}{\sin^4 E_{21}^M} - \frac{2\rho_2 C_{21} C_{22}}{\sin^2 E_{21}^M \sin^2 E_{22}^M} + \frac{C_{22}^2}{\sin^4 E_{22}^M} \right] \right\} . \tag{40}$$

In general, the maximum elevation angle is not the specified parameter in the satellite laser ranging process. Therefore, Equation (40) must be

modified to become a function of some known parameters such as the minimum elevation angle and the orbit separation before we can examine its properties. To illustrate this, Equation (40) is evaluated for the special case where the two ground stations are equidistant from the x-axis.

In this special case, let the satellite orbits be $\ell/2$ away from the $y = 0$ plane, and the two ground stations be equidistant from the x-axis. The baseline distance is B_L. This geometry is illustrated in Figure 4.

In order to acquire the same number of range measurements on the two passes, the threshold elevation angles between these passes must be different, i.e., $E^0_{m1} \neq E^0_{m2}$. By referring to Figure 2, the specified minimum elevation angle (E_{min}) of the ranging geometry must be equal to the threshold elevation angle formed by a station and a satellite path farther away from that station. That is,

$$E^0_{11} = E^0_{22} = E_{min} \quad . \tag{41}$$

The remaining threshold elevation angles can be found as

$$E^0_{12} = E^0_{21} = \tan^{-1}\left[\frac{h \tan E_{min}}{(h^2 - \ell B_L \cos\gamma \tan^2 E_{min})^{1/2}}\right] \quad . \tag{42}$$

The sine of the various maximum elevation angles can be expressed as

$$\sin E^M_{11} = \sin E^M_{22} = \frac{h}{[h^2 + 1/4(B_L \cos\gamma - \ell)^2]^{1/2}} \, , \tag{43}$$

and

$$\sin E^M_{12} = \sin E^M_{21} = \frac{h}{[h^2 + 1/4(B_L \cos\gamma - \ell)^2]^{1/2}} \quad . \tag{44}$$

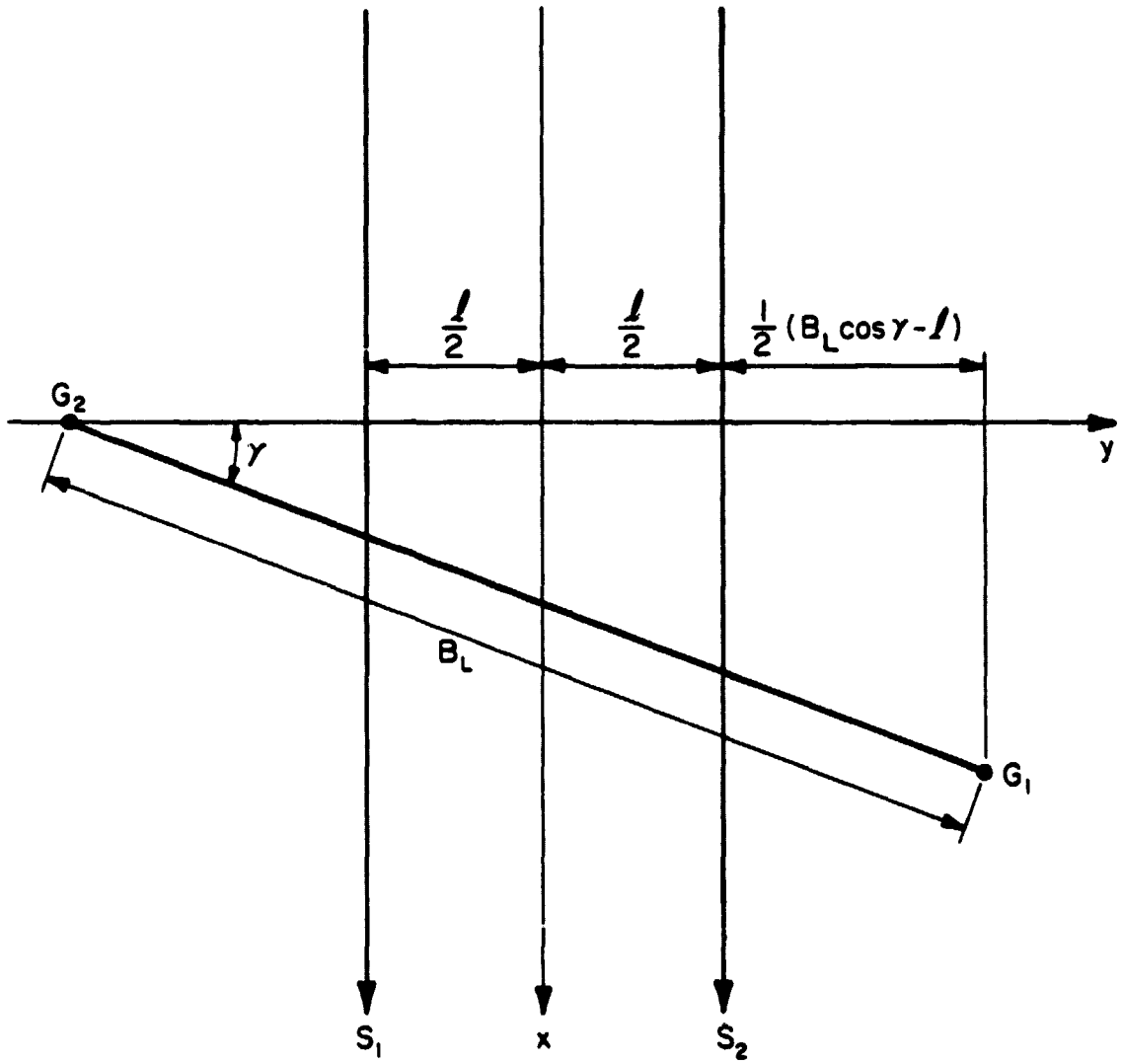

Figure 4. Ranging geometry for the case where the two ground stations are equidistant from the x-axis.

By using the results of Equations (41) through (44), the equalities

$$\frac{\sin^2 E_{11}^M \sin^2 E_{12}^M}{\sin^2(E_{11}^M - E_{12}^M)} = \frac{\sin^2 E_{21}^M \sin^2 E_{22}^M}{\sin^2(E_{21}^M - E_{22}^M)} = \frac{h^2}{\ell^2} \quad , \tag{45}$$

and

$$C_{11} = C_{22} \quad , \quad C_{12} = C_{21} \quad . \tag{46}$$

can be derived.

By substituting Equations (43) through (46) into Equation (40) and taking the square roots on both sides, an expression for the rms baseline error can be obtained as

$$\sigma_{B_L} = \langle \Delta B_L^2 \rangle^{1/2} = \frac{\sqrt{2}\,\sigma_\beta \cos\gamma}{\ell h} \{C_{11}^2[h^2 + 1/4(B_L \cos\gamma + \ell)^2]^2$$

$$- (\rho_1 + \rho_2)\, C_{11}C_{12}[h^2 + 1/4(B_L \cos\gamma + \ell)^2][h^2 + 1/4(B_L \cos\gamma - \ell)^2]$$

$$+ C_{12}^2[h^2 + 1/4(B_L \cos\gamma - \ell)^2]^2\}^{1/2} \quad . \tag{47}$$

In order to relate the baseline error directly to the atmospheric refraction error, Equation (47) is normalized by the maximum atmospheric refraction error ($\sigma_{AR} = \frac{\sigma_\beta}{\sin E_{min}}$, the refraction error for the minimum elevation angle). This gives

$$\frac{\sigma_{B_L}}{\sigma_{AR}} = \frac{\sqrt{2} \cos\gamma \sin E_{min}}{\ell h} \{C_{11}^2[h^2 + 1/4(B_L \cos\gamma + \ell)^2]^2$$

$$- (\rho_1 + \rho_2)\, C_{11}C_{12}[h^2 + 1/4(B_L \cos\gamma + \ell)^2][h^2 + 1/4(B_L \cos\gamma - \ell)^2]$$

$$+ C_{12}^2[h^2 + 1/4(B_L \cos\gamma - \ell)^2]^2\}^{1/2} \tag{48}$$

where $\frac{\sigma_{B_L}}{\sigma_{AR}}$ is a dimensionless parameter called the baseline error

multiplier. When the maximum refraction error (σ_{AR}) is multiplied by this multiplier, the magnitude of the rms baseline error can be obtained.

Equation (48) indicates that the baseline error is smaller for the higher correlation of refraction errors on the two passes, and vice versa. In all cases, the baseline error is an increasing function of the baseline distance, and is proportional to cos γ.

The increasing characteristic of the baseline error with respect to the baseline distance can be explained by observing that the increase in baseline distance causes an increase in the station-to-satellite distances. Increasing the station-to-satellite distances will result in larger range measurement errors. Consequently, the baseline error, which depends solely on the range measurement errors, will also be increased.

The dependence of baseline error on angle γ can be explained by observing that the baseline error includes only the y-coordinate errors. The z-coordinate errors contribute second-order effects which are not included in this analysis. By keeping the other parameters constant, the closer γ approaches 0°, the longer the y-coordinate baseline will be, which will result in a larger baseline error. When γ equals 90°, the y-coordinate baseline will be zero. As a result, the corresponding baseline error will be zero.

An approximate lower bound for the baseline error can be found by assuming a zero baseline and letting C_{mn} be unity. This yields

$$\frac{\sigma_{B_L}}{\sigma_{AR}} \geq \sqrt{2} \cos \gamma \sin E_{min} [2 - (\rho_1 + \rho_2)]^{1/2} \left[\frac{h}{\ell} + \frac{\ell}{4h} \right] . \qquad (49)$$

Inequality (49) shows the dependence of baseline error on the orbit geometry explicitly. It also indicates that a baseline error of zero for

an arbitrary geometry can only be achieved when the refraction errors on the two passes are perfectly correlated.

4.2 Baseline Error for the Uncorrelated-Path Laser Ranging

When the ground stations have undergone large fluctuations in surface pressure, temperature and water vapor pressure on the two satellite passes, a zero correlation of meteorological data errors on the two passes will be expected. Consequently, the atmospheric refraction error on the two passes will also be uncorrelated. This implies that

$$\rho_m = 0 \qquad m = 1,2 \quad . \tag{50}$$

We refer to this configuration as the uncorrelated-path ranging. The normalized rms baseline error for this configuration can be obtained by substituting Equation (50) into Equation (48). This yields

$$\frac{\sigma_{B_L}}{\sigma_{AR}}\,(\text{uncorr}) = \frac{\sqrt{2}\,\cos\gamma\,\sin E_{min}}{\ell h}\,\{C_{11}^2[h^2 + 1/4(B_L\cos\gamma + \ell)^2]^2$$

$$+ C_{12}^2[h^2 + 1/4(B_L\cos\gamma - \ell)^2]^2\}^{1/2} \quad . \tag{51}$$

By substituting Equation (50) into Inequality (49), we can express the lower bound for the baseline error in the uncorrelated-path ranging system as

$$\frac{\sigma_{B_L}}{\sigma_{AR}}\,(\text{uncorr}) \geq 2\cos\gamma\,\sin E_{min}\left[\frac{h}{\ell} + \frac{\ell}{4h}\right] \quad . \tag{52}$$

Inequality (52) indicates that a nonzero baseline error is always present (except when γ equals 90°) no matter how small the baseline is.

The baseline distance is limited by the fact that both satellite passes must be visible at both ground stations. Consequently, the baseline distance cannot be exceeded by the value

$$B_{Lmax} = \left(\frac{2h}{\tan E_{min}} - \ell \right) \frac{1}{\cos \gamma} \quad . \tag{53}$$

With the result of Equation (53), we can find the upper bound for the baseline error as

$$\frac{\sigma_{B_L}}{\sigma_{AR}} \text{(uncorr)} < \frac{8h \cos \gamma}{3\ell \sin E_{min}} \quad . \tag{54}$$

The normalized rms baseline errors for the uncorrelated-path laser ranging system versus the baseline distance are plotted in Figures 5 through 13 for different sets of parameters. As expected, these plots indicate that the baseline error is an increasing function of the baseline distance; and it is a cosine function of the angle γ.

The exact dependence of baseline error on the orbit separation and the orbit altitude is very difficult to see in general. But for the short baseline ranging, the baseline error is shown by Inequality (52) to be related to the two parameters according to $\left(\frac{h}{\ell} + \frac{\ell}{4h} \right)$, and the minimum baseline error can be achieved when the orbit separation is twice as much as the orbit altitude, i.e., $\ell = 2h$. This property is well illustrated in Figures 5 and 8 where the orbit separation of 1000 km gives the smallest baseline error. For the long baseline ranging, the baseline error is shown by Inequality (54) to increase directly with the orbit altitude and inversely with the orbit separation. These properties are illustrated in Figures 5 through 13. In all cases, the range measurements must be taken at two widely separated satellite orbits in order to strengthen the geometry sufficiently to recover the stations and the baseline at the centimeter level [10].

The dependence of baseline error on the minimum elevation angle cannot be extracted directly from Figures 5 through 13 because the normalization

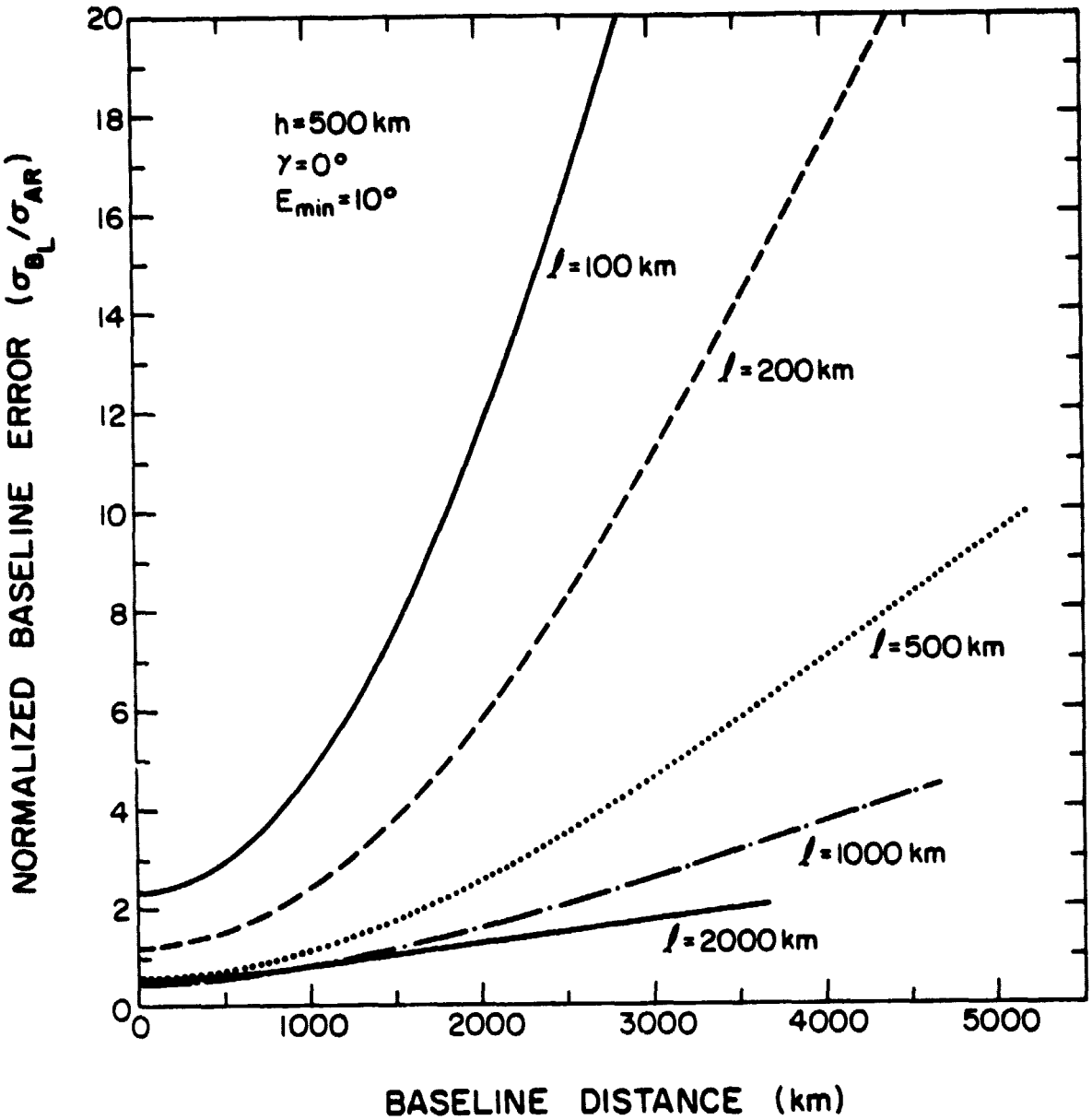

Figure 5. Normalized baseline error versus baseline for different satellite orbit separations in the uncorrelated-path laser ranging system.

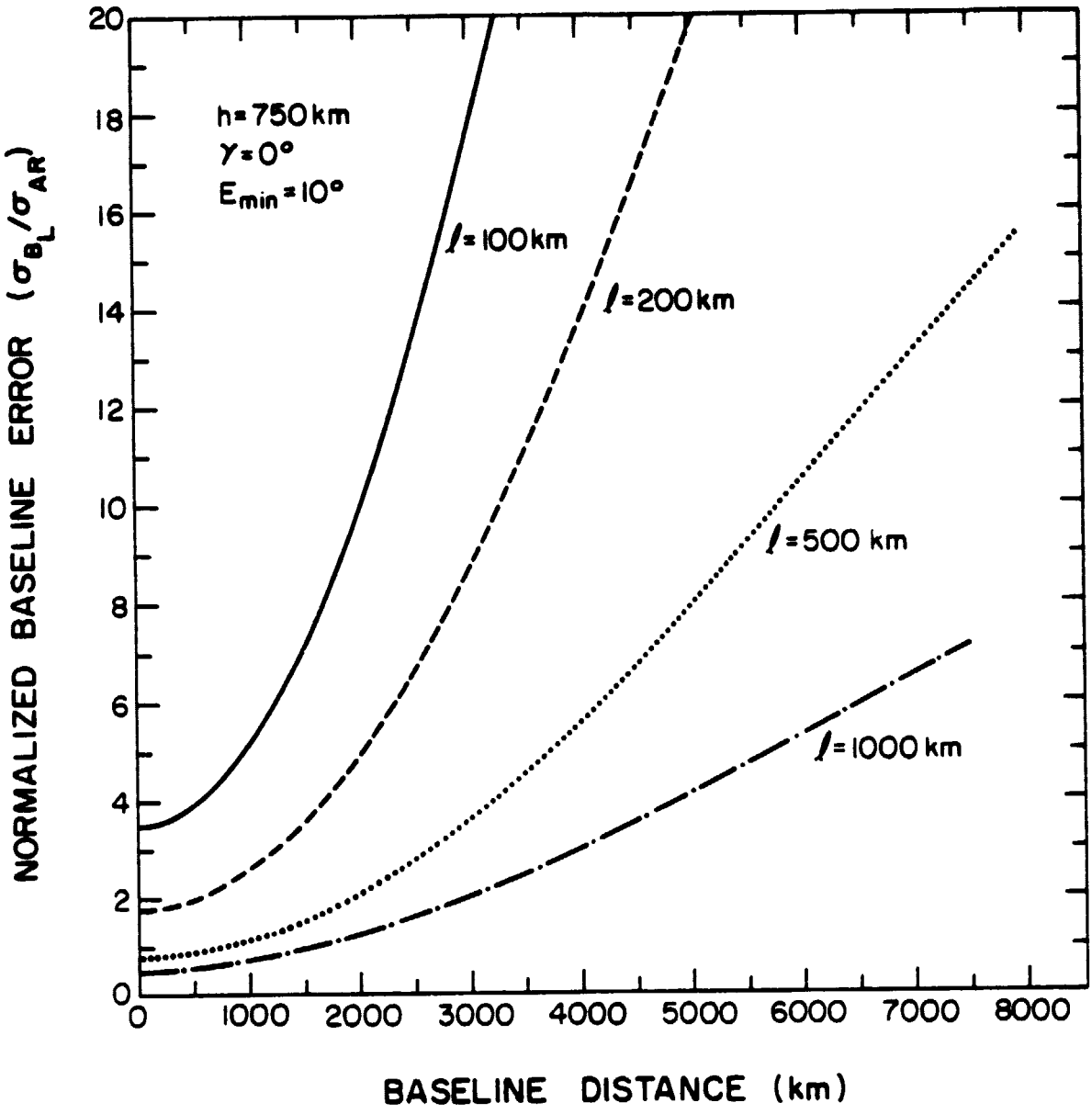

Figure 6. Normalized baseline error versus baseline for different satellite orbit separations in the uncorrelated-path laser ranging system.

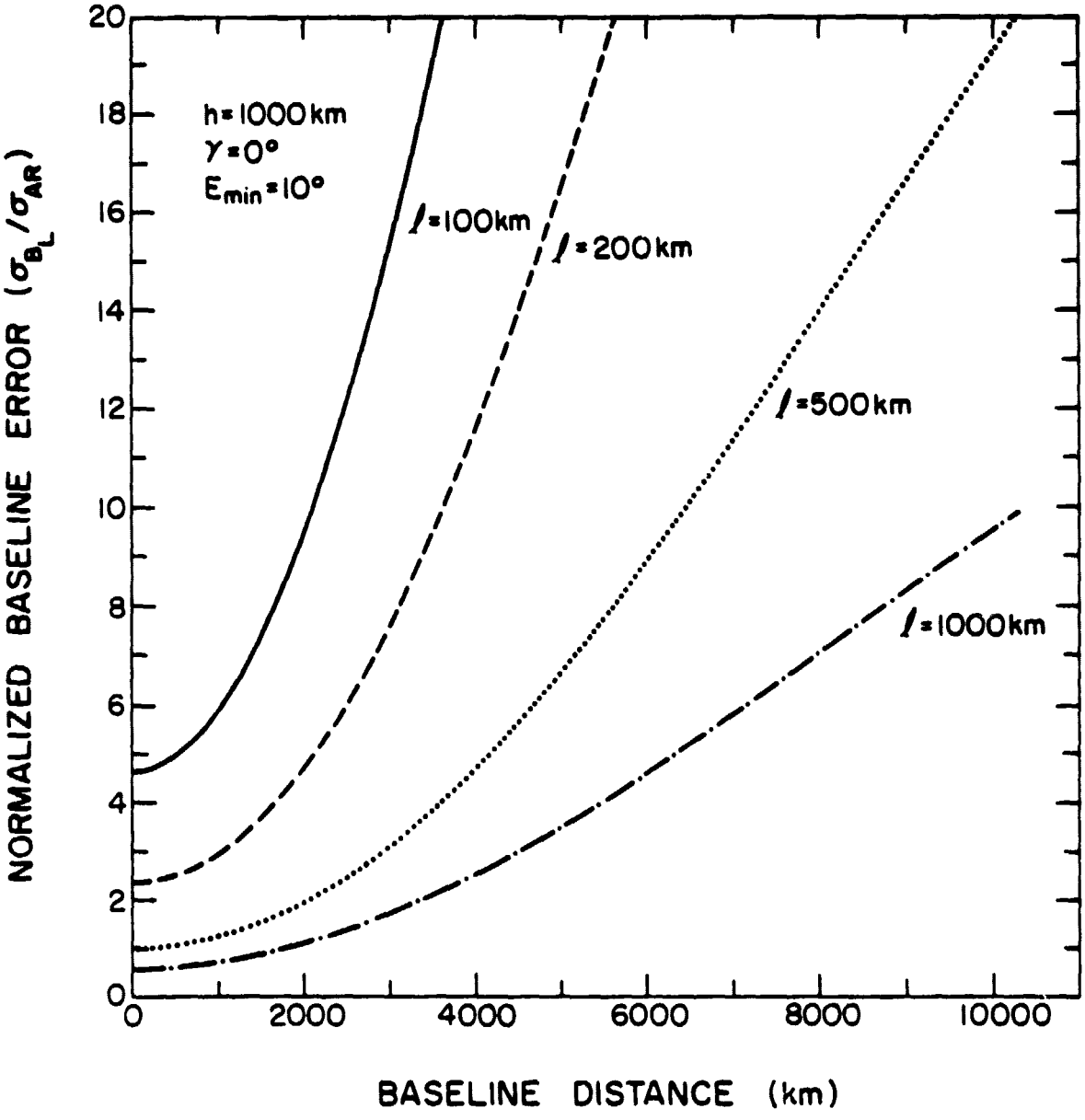

Figure 7. Normalized baseline error versus baseline for different satellite orbit separations in the uncorrelated-path laser ranging system.

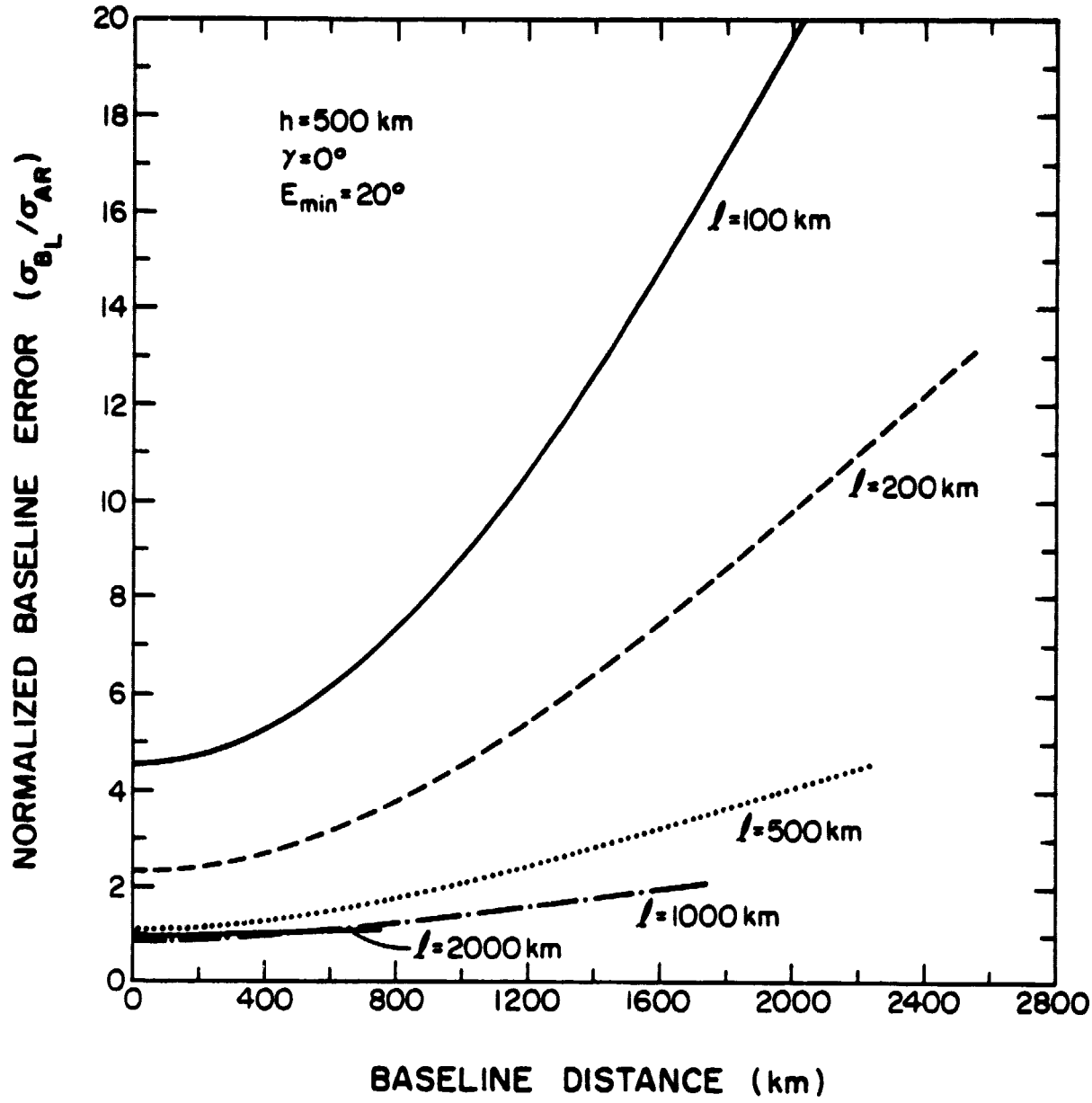

Figure 8. Normalized baseline error versus baseline for different satellite orbit separations in the uncorrelated-path laser ranging system.

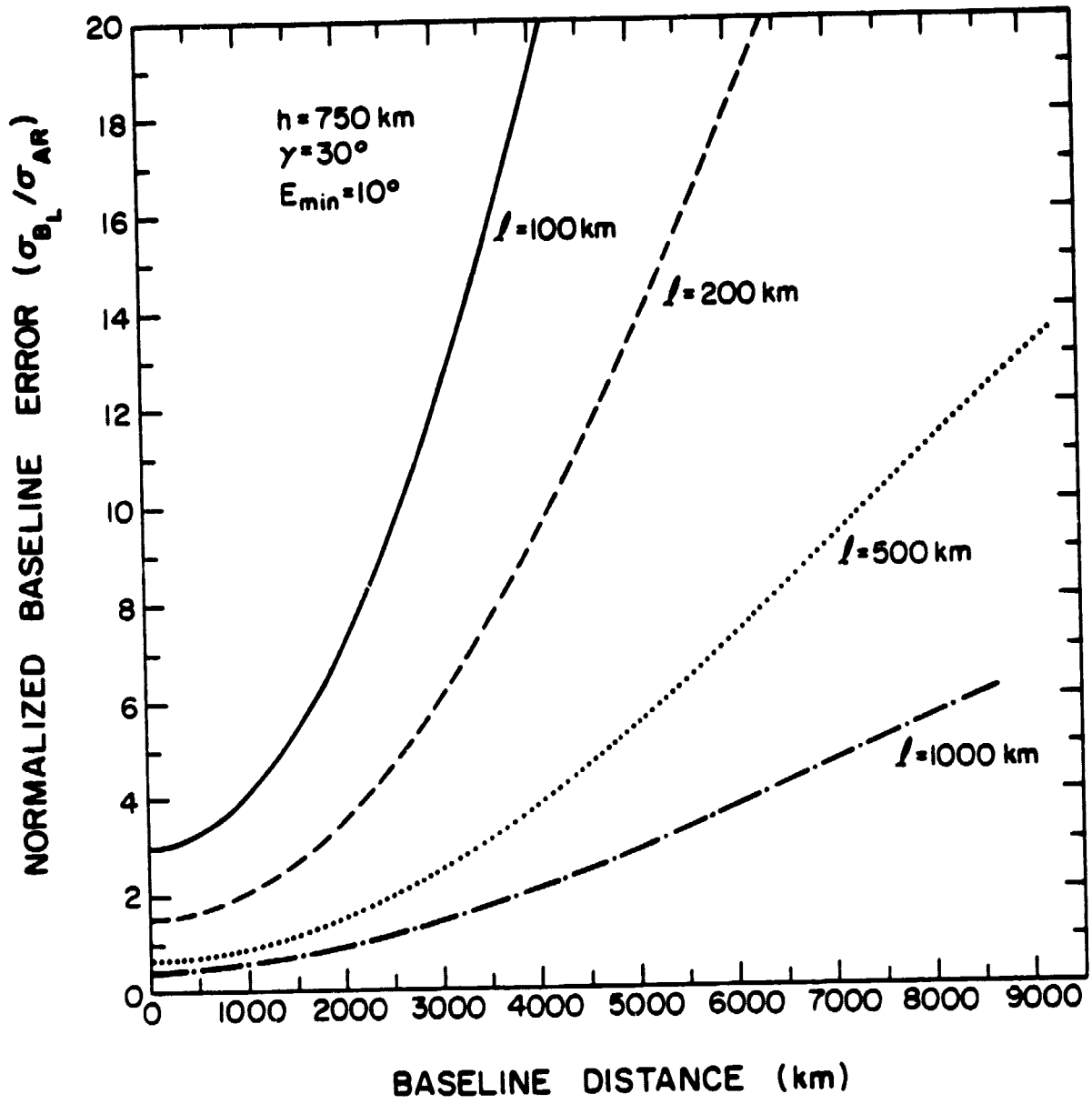

Figure 9. Normalized baseline error versus baseline for different satellite orbit separations in the uncorrelated-path laser ranging system.

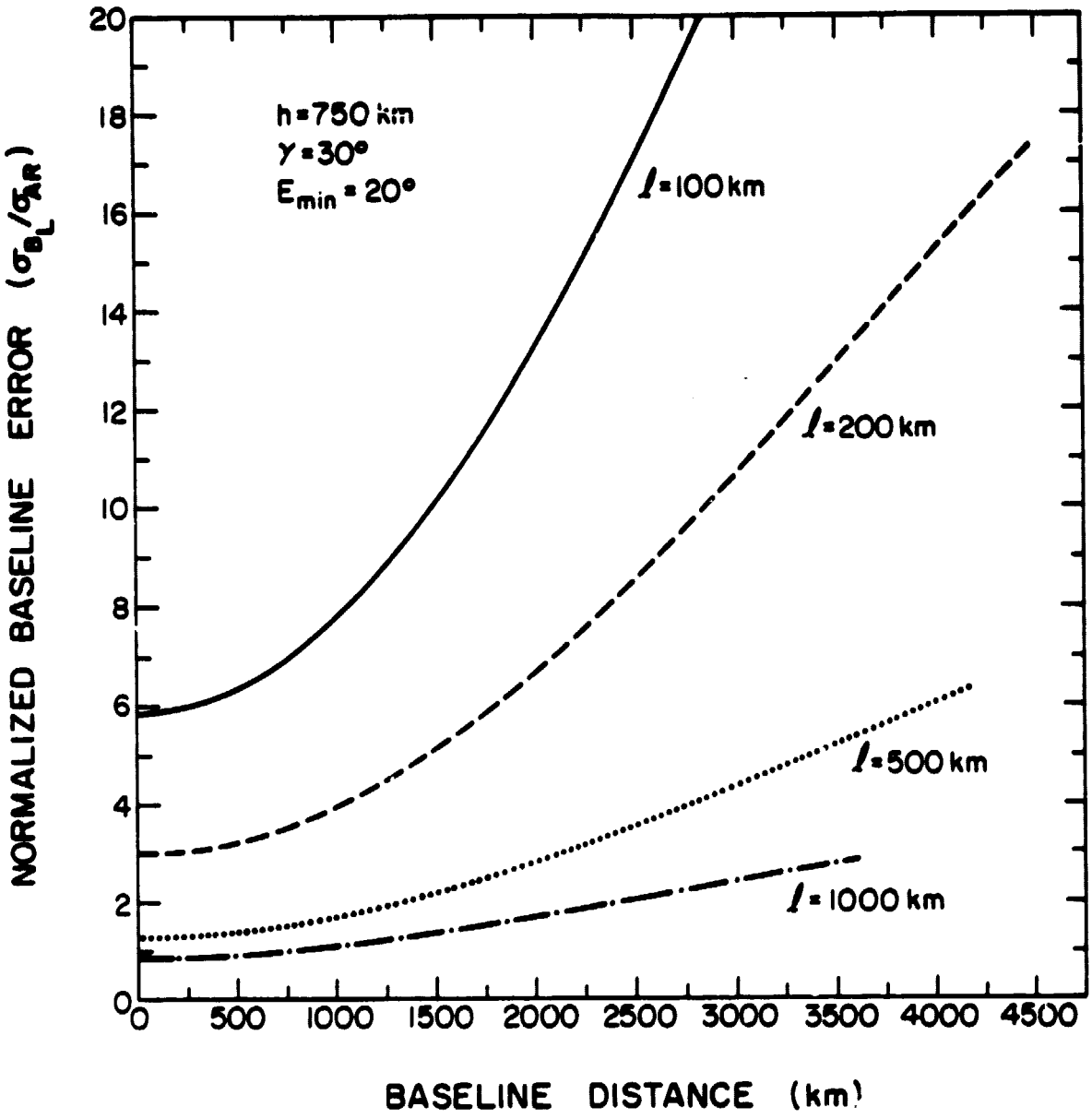

Figure 10. Normalized baseline error versus baseline for different satellite orbit separations in the uncorrelated-path laser ranging system.

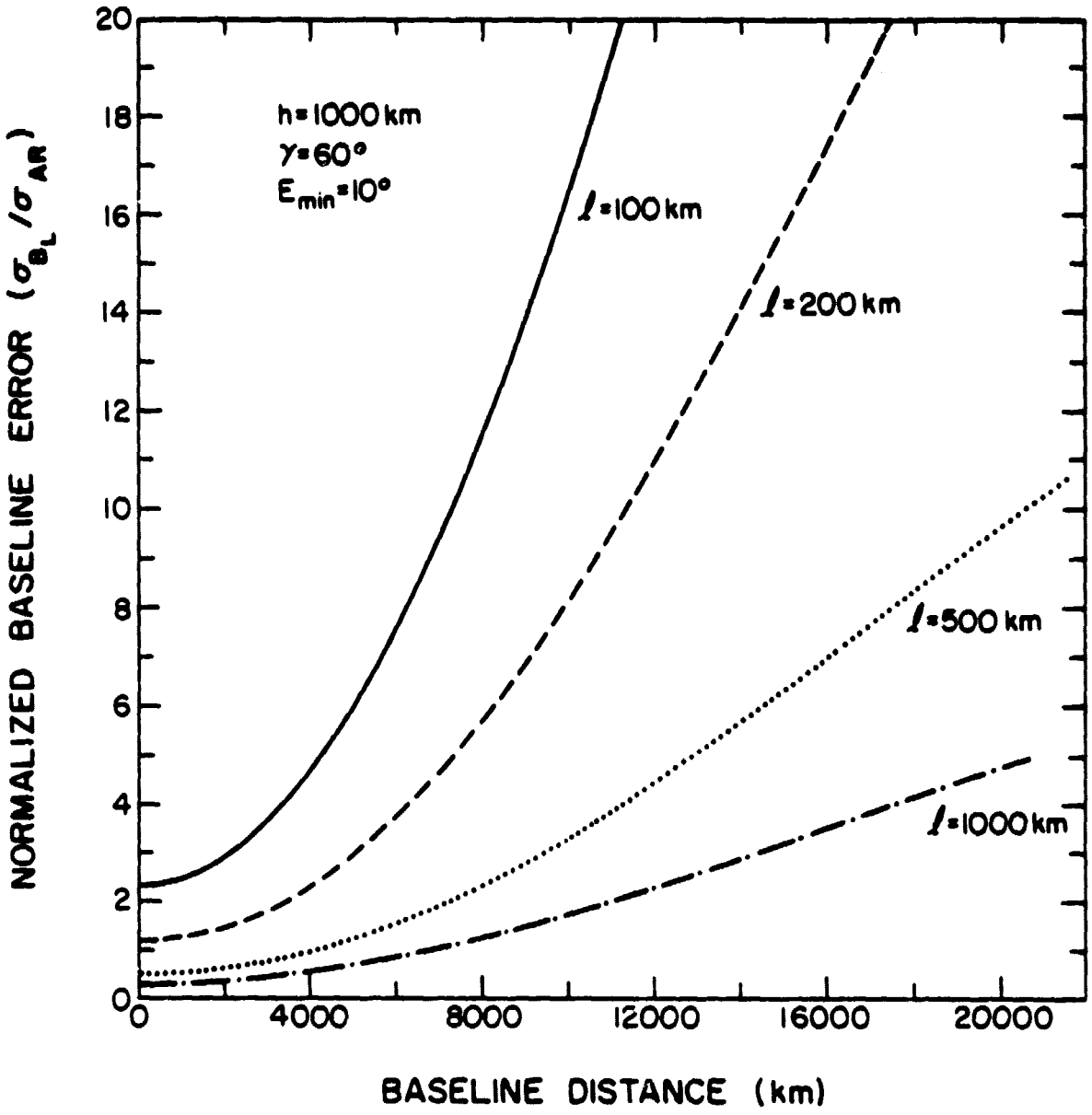

Figure 11. Normalized baseline error versus baseline for different satellite orbit separations in the uncorrelated-path laser ranging system.

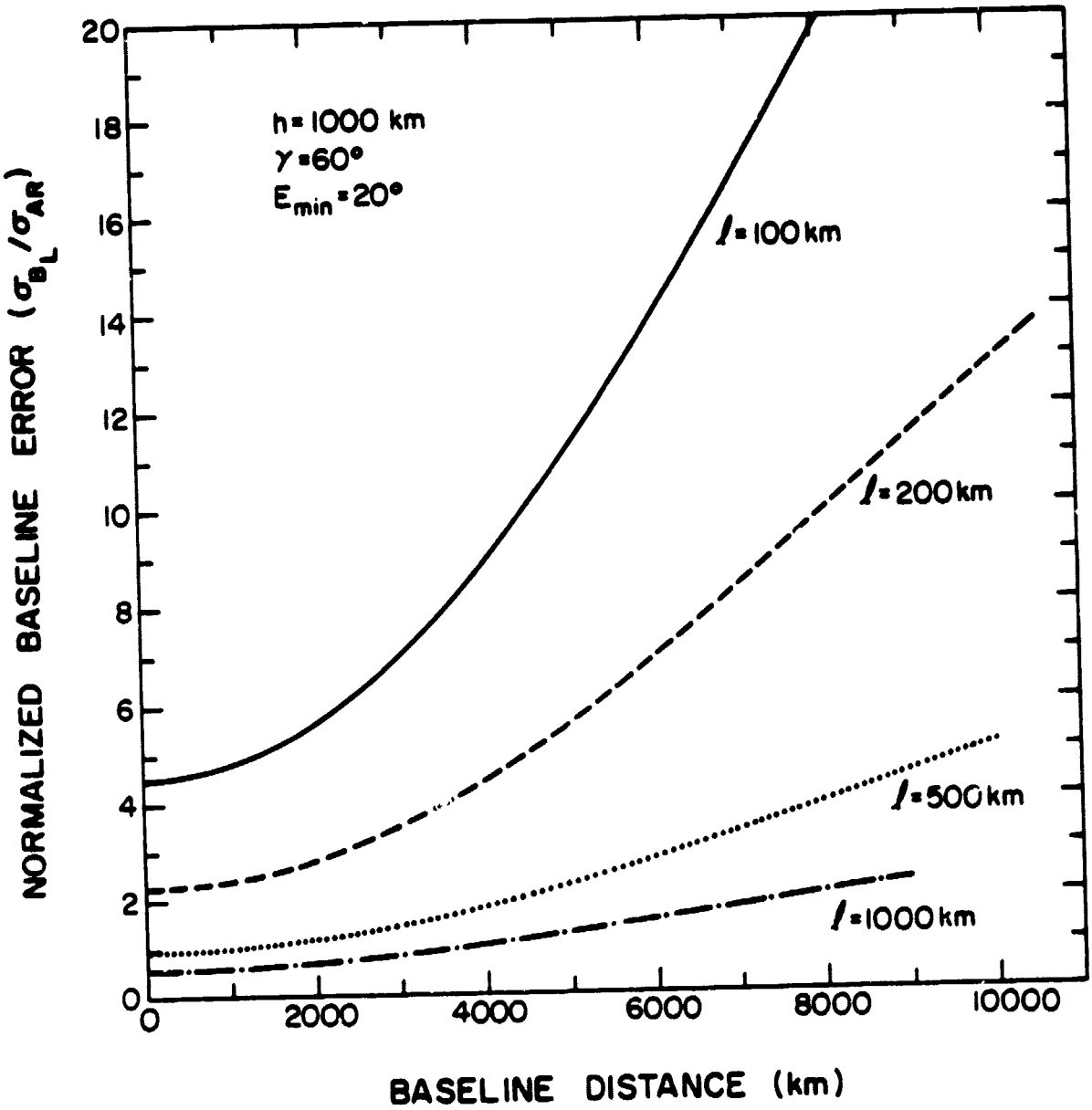

Figure 12. Normalized baseline error versus baseline for different satellite orbit separations in the uncorrelated-path laser ranging system.

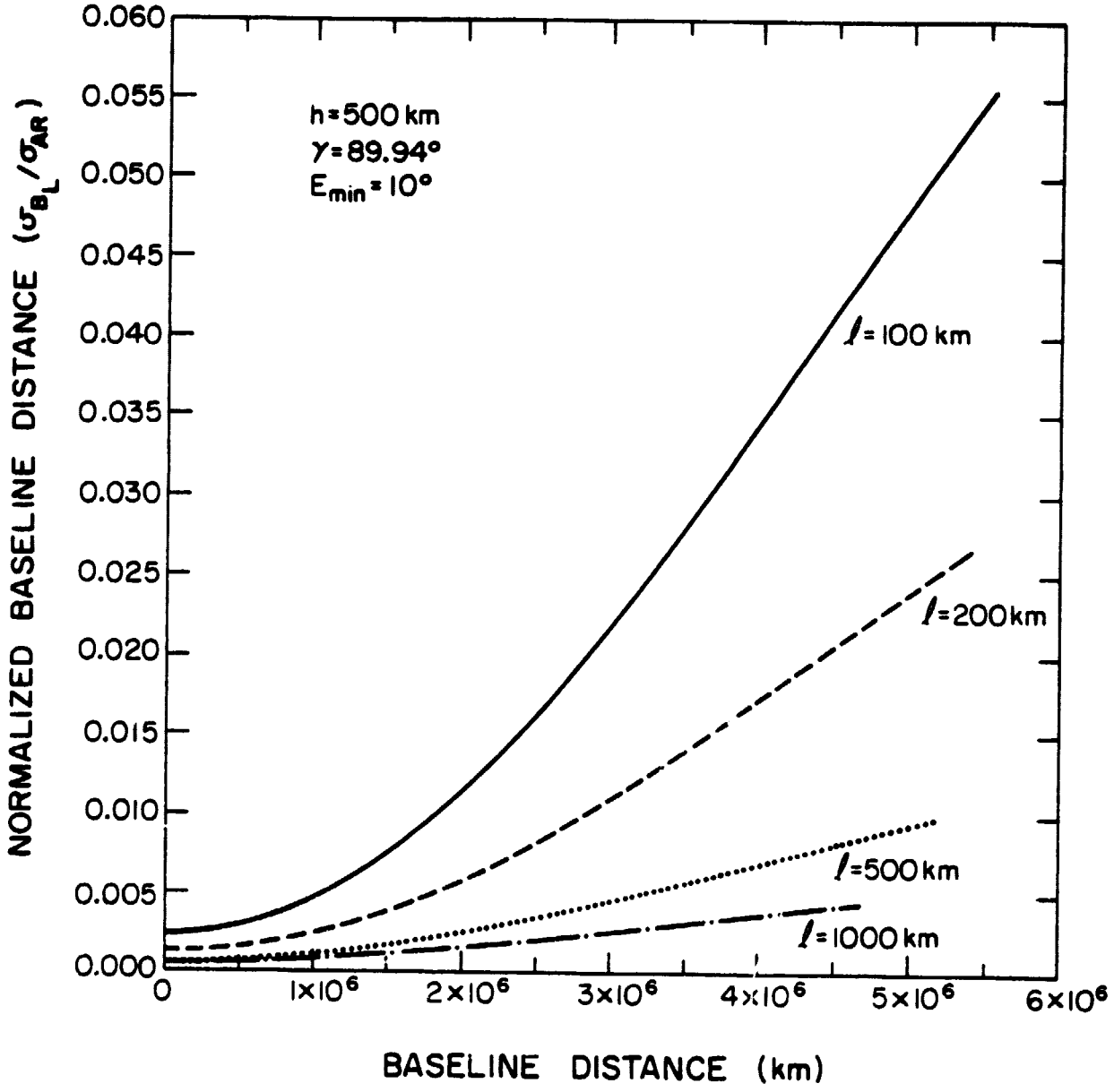

Figure 13. Normalized baseline error versus baseline for different satellite orbit separations in the uncorrelated-path laser ranging system.

factor used in Equation (51) involves the minimum elevation angle which varies for different sets of parameters. In order to investigate this relationship, the absolute rms baseline error (σ_{B_L}) is plotted versus the baseline distance for various minimum elevation angles (E_{min}) in Figure 14; and σ_{B_L} versus E_{min} is plotted in Figure 15 for various baseline distances. These plots indicate that the baseline error is a decreasing function of the minimum elevation angle. This relationship between the baseline error and the minimum elevation angle can be explained by the fact that while keeping the other parameters constant, the increase in minimum elevation angle will result in the shorter satellite-to-ground-station distance. Consequently, the range measurement errors, and hence the baseline error, will be smaller.

In most cases the orbit altitude and the minimum elevation angle are usually defined prior to the actual ranging, so the baseline error depends very much on the orbit separation for a given baseline ranging. For example, the altitudes for many of the satellite orbits are 1000 km. For a minimum elevation angle of 20° and an angle γ of 60°, the 1000-km baseline has a rms error of around 0.5 σ_{AR} for a 1000-km orbit separation and a rms error of around 5 σ_{AR} for a 100-km orbit separation (refer to Figure 2). This effect of orbit separation on the baseline error will even be more pronounced for a longer baseline.

4.3 Baseline Error for the Correlated-Path Laser Ranging

If the weather conditions in both ground stations during the second satellite pass are almost the same as those during the first satellite pass, we would expect the atmospheric refraction to be highly correlated. This implies that

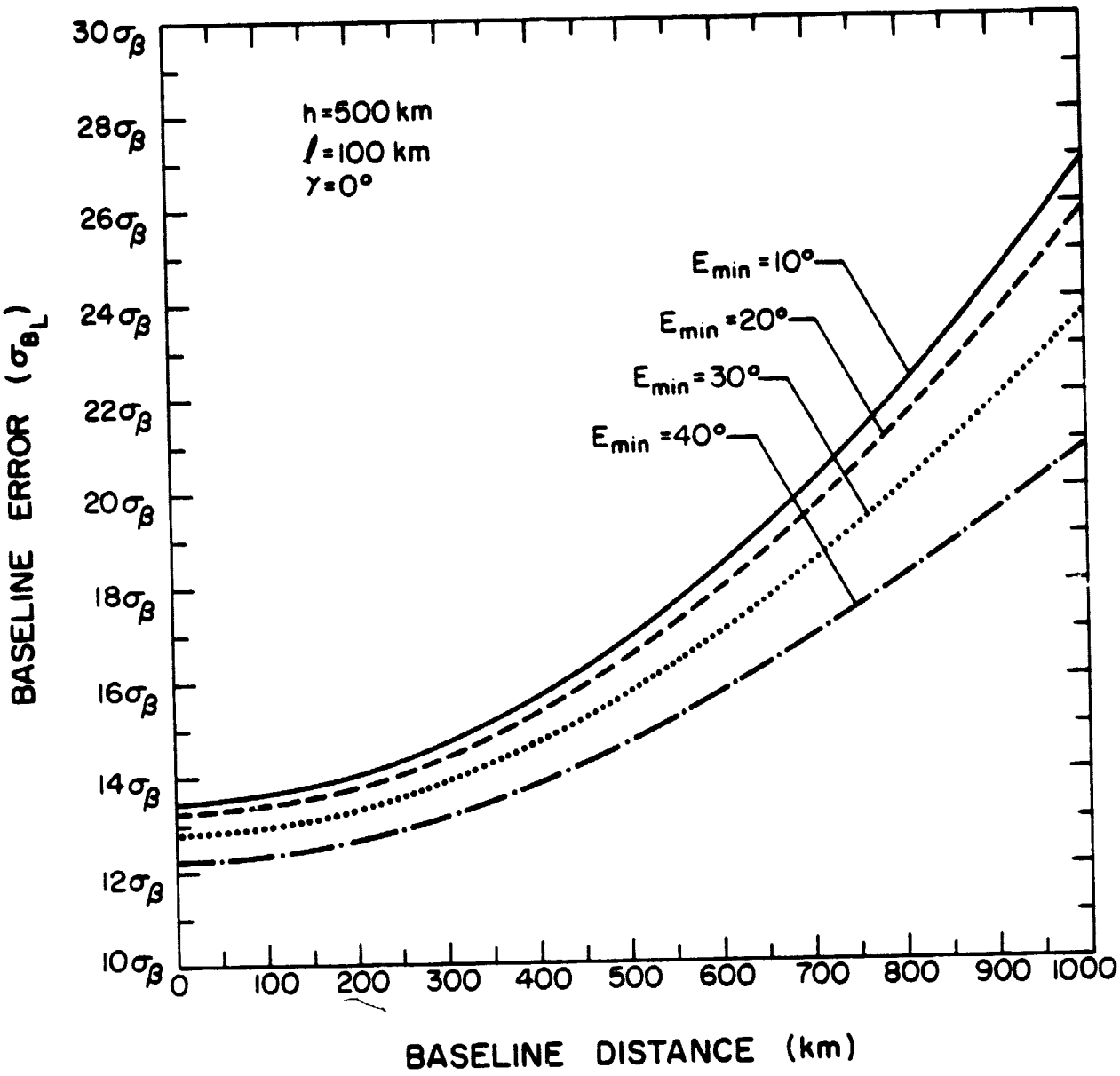

Figure 14. Baseline error versus baseline for different elevation angles in the uncorrelated-path laser ranging system.

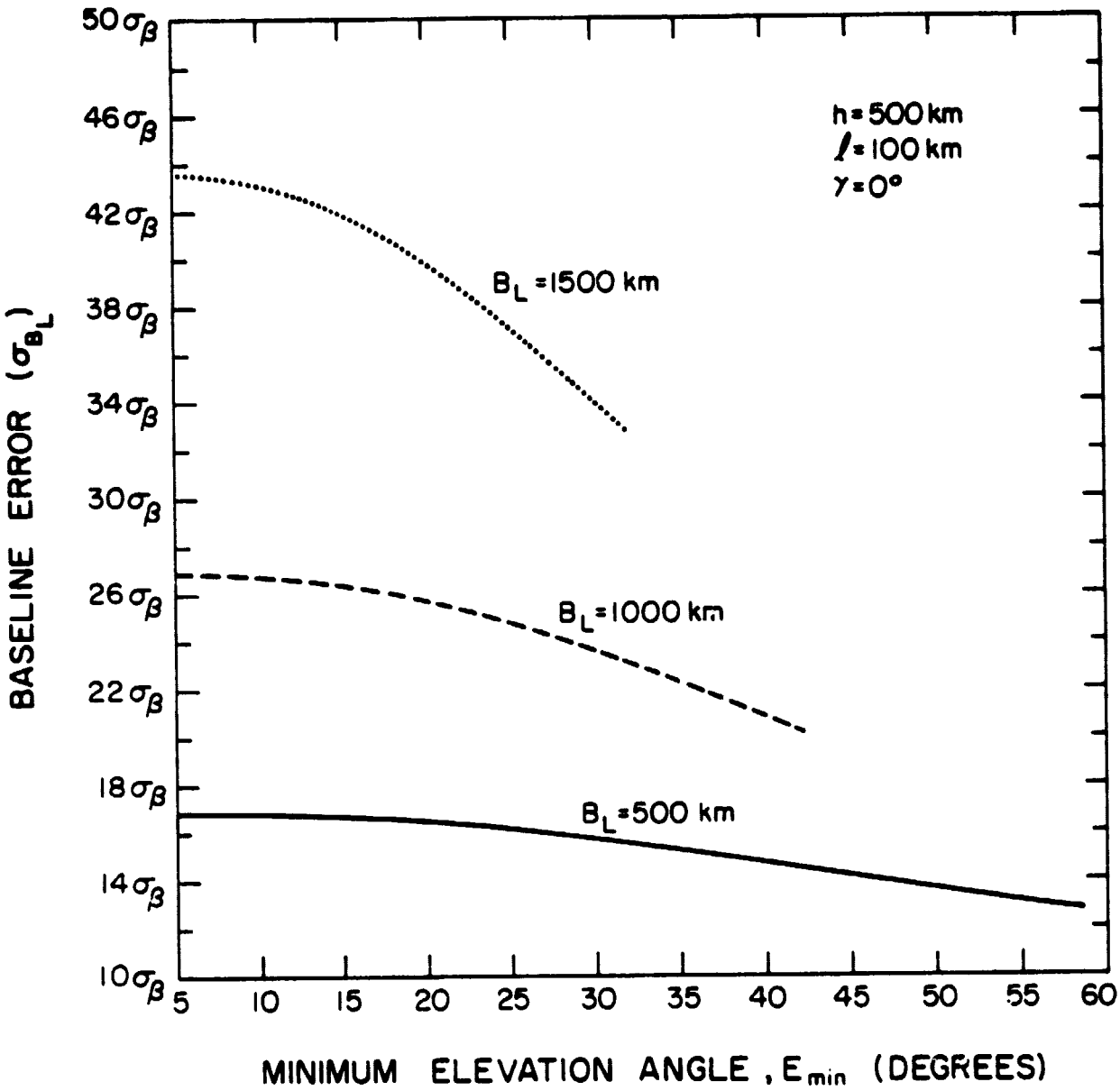

Figure 15. Baseline error versus minimum elevation angle for different baselines in the uncorrelated-path laser ranging system.

$$\rho_m = 1 \qquad m = 1,2 \quad . \tag{55}$$

We refer to this configuration as the correlated-path ranging. The absolute and normalized rms baseline errors for this configuration can be obtained by substituting Equation (55) into Equations (47) and (48). This yields, respectively,

$$\sigma_{B_L}(\text{corr}) = \frac{\sqrt{2}\,\sigma_\beta \cos\gamma}{\ell h}\{C_{11}[h^2+1/4(B_L\cos\gamma+\ell)^2]-C_{12}[h^2+1/4(B_L\cos\gamma-\ell)^2]\} \tag{56}$$

and

$$\frac{\sigma_{B_L}}{\sigma_{AR}}(\text{corr}) = \frac{\sqrt{2}\cos\gamma\sin E_{min}}{\ell h}\{C_{11}[h^2+1/4(B_L\cos\gamma+\ell)^2]$$

$$- C_{12}[h^2+1/4(B_L\cos\gamma-\ell)^2]\} \quad . \tag{57}$$

By substituting Equation (55) into Equation (49), we find that the minimum baseline error of zero can be achieved when $B_L = 0$.

By referring to Equation (53), the upper bound for the baseline error in this system can be found as

$$\frac{\sigma_{B_L}}{\sigma_{AR}}(\text{corr}) < \frac{\sqrt{2}\,h\cos\gamma}{3\,\ell\sin E_{min}} + \frac{\sqrt{2}\,B_{Lmax}\cos^2\gamma\sin E_{min}}{h} \quad . \tag{58}$$

Since B_{Lmax} increases with the orbit altitude (h) and decreases with the orbit separation (ℓ), Inequality (58) indicates that the baseline error in this case also increases directly with the orbit altitude and inversely with the orbit separation for long baselines.

Equation (56) is plotted versus the baseline distance for four different minimum elevation angles in Figure 16; and it is plotted versus

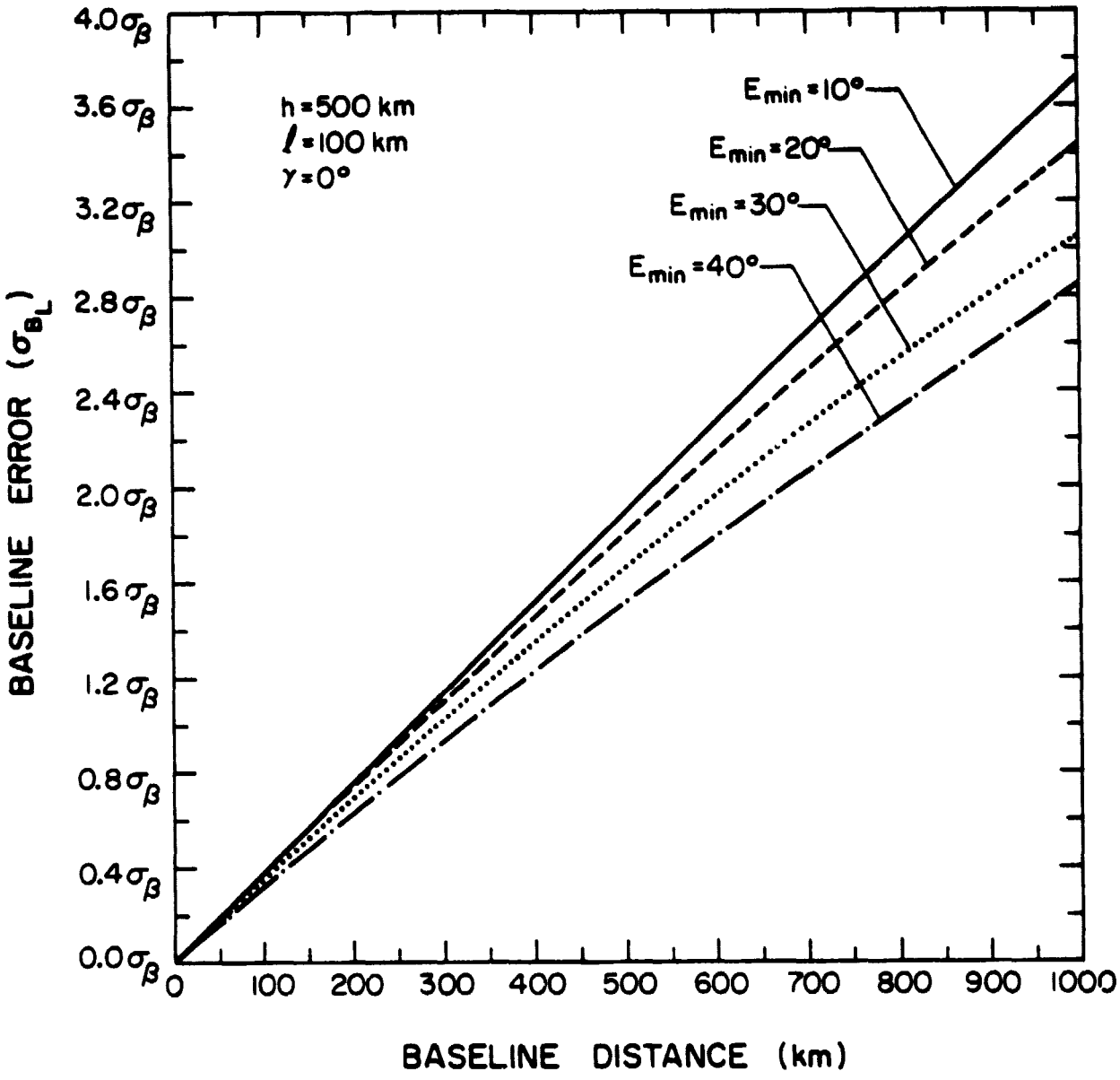

Figure 16. Baseline error versus baseline for different elevation angles in the correlated-path laser ranging system.

the minimum elevation angle in Figure 17 to illustrate the dependence of baseline error on minimum elevation angle. Equation (57) is plotted versus the baseline distance in Figures 18 through 21 for different sets of orbit separations, orbit altitudes, minimum elevation angles and the γ angles. These plots indicate that the general properties of the baseline error mentioned in Section 4.2 have also held true here for the correlated-path ranging. This is to be expected because the geometric model used in this section, on which these properties are based, is the same as that used in Section 4.2.

It is interesting to note the importance of atmospheric refraction error correlation in the satellite laser ranging process. By referring to Equation (47), we see that the higher the correlation between the refraction errors on the two passes, the lower the baseline error. In particular, the baseline error for the uncorrelated-path ranging can be more than an order of magnitude higher than that for the correlated-path ranging. Since the correlation between refraction errors on the two passes depends very much on the temporal separation between these passes, it is important to keep the [illegible] between passes short enough in order to enhance the refraction error correlation.

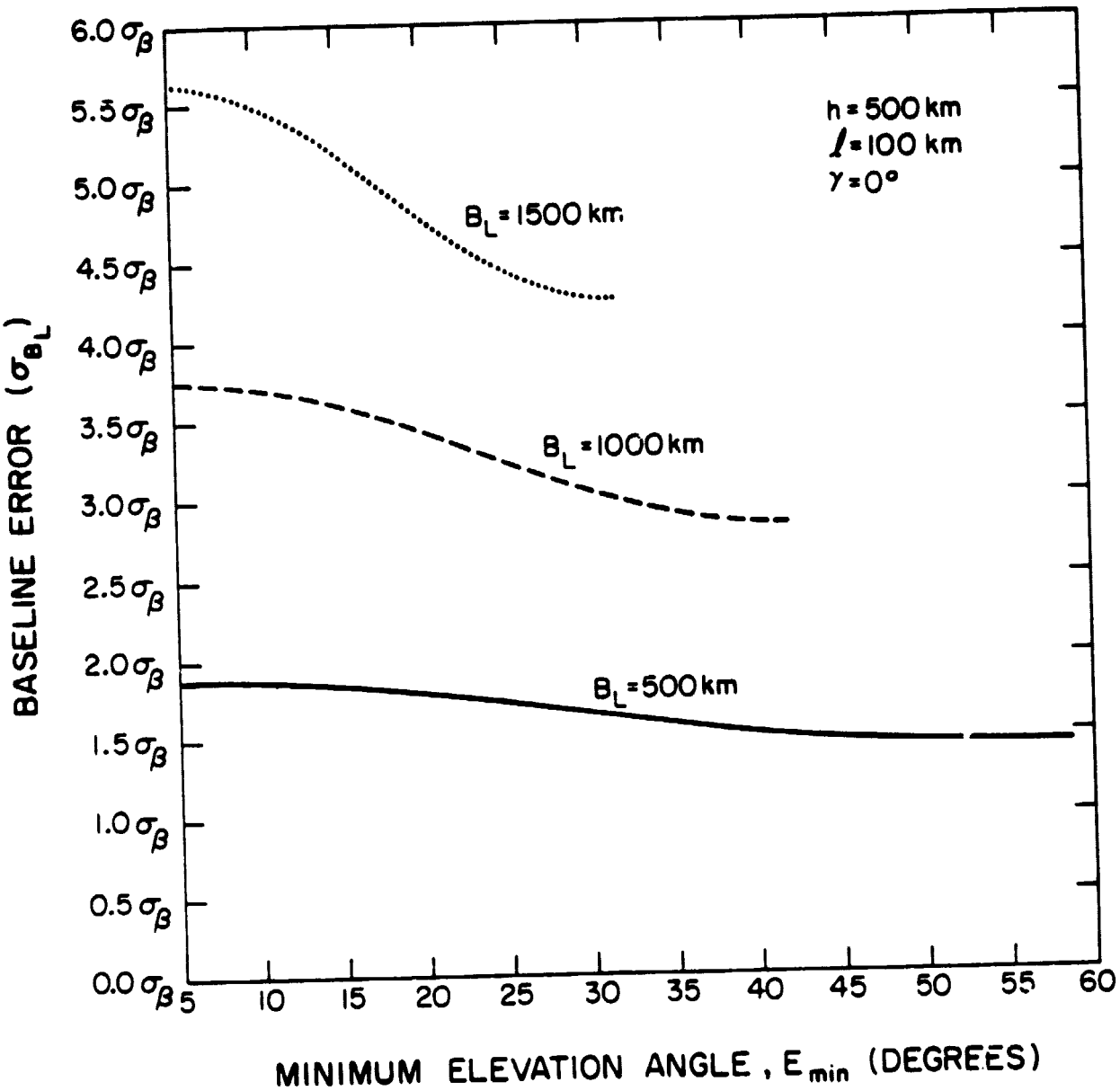

Figure 17. Baseline error versus minimum elevation angle for different baselines in the correlated-path laser ranging system.

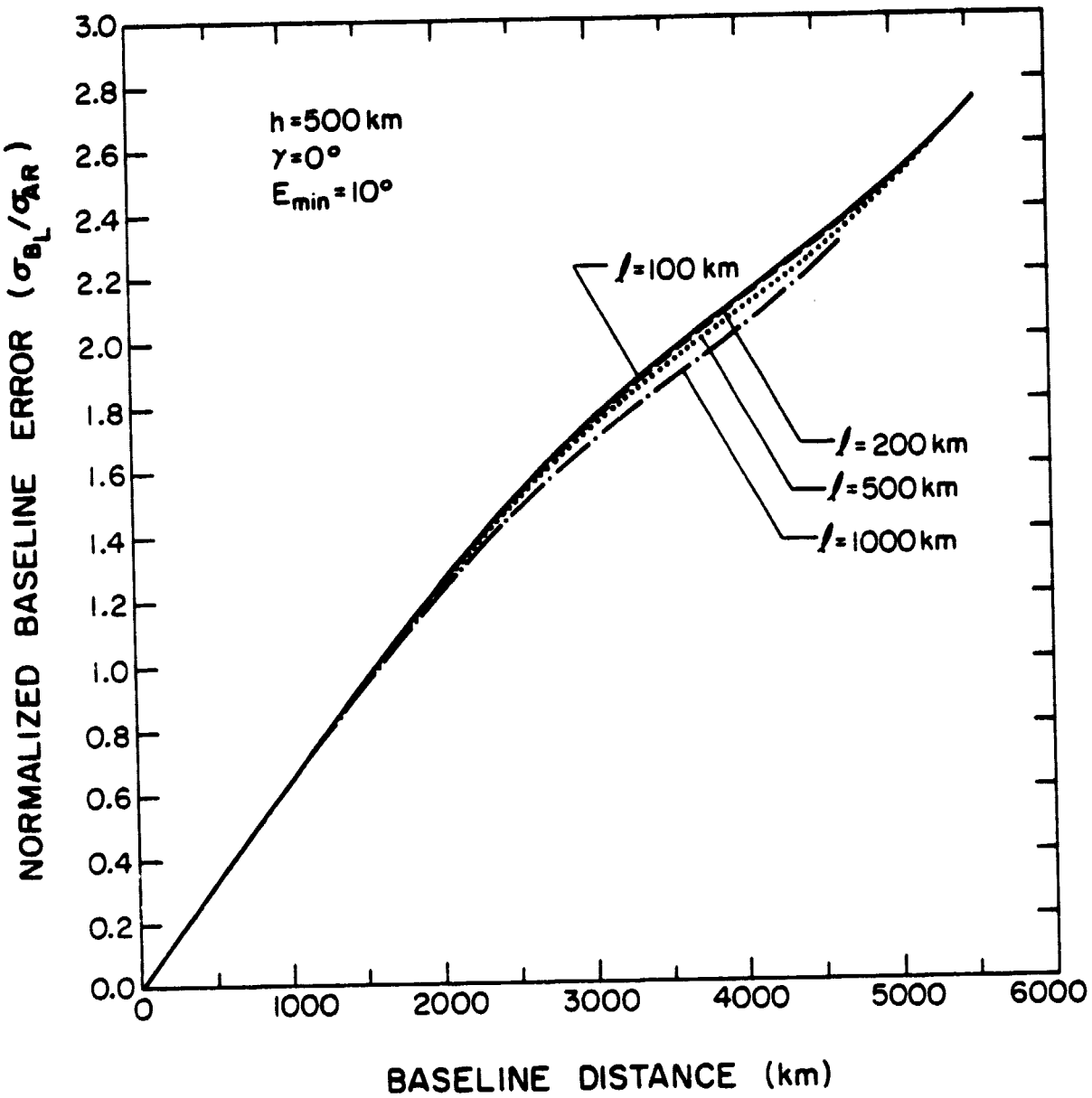

Figure 18. Normalized baseline error versus baseline for different satellite orbit separations in the correlated-path laser ranging system.

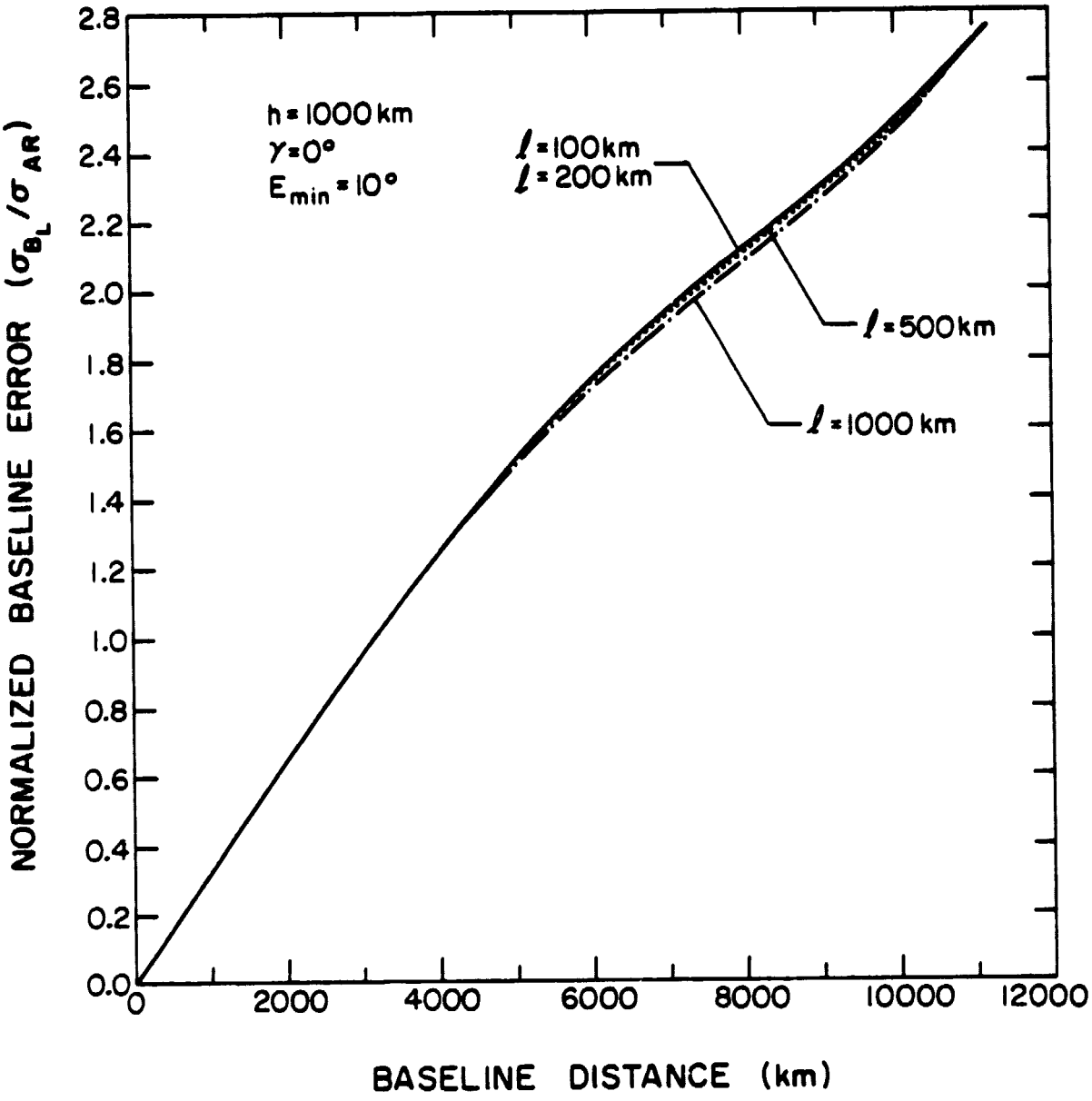

Figure 19. Normalized baseline error versus baseline for different satellite orbit separations in the correlated-path laser ranging system.

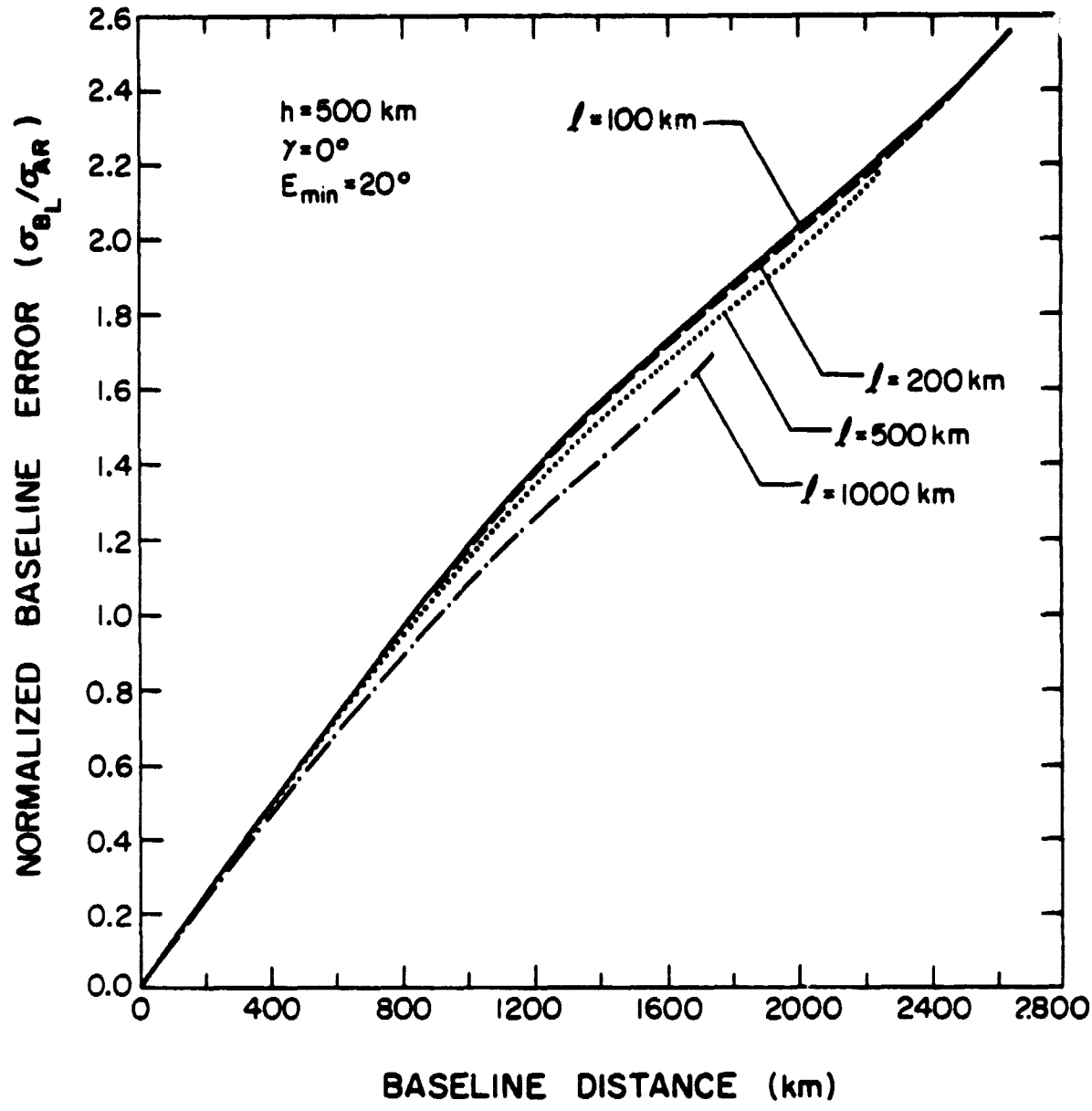

Figure 20. Normalized baseline error versus baseline for different satellite orbit separations in the correlated-path laser ranging system.

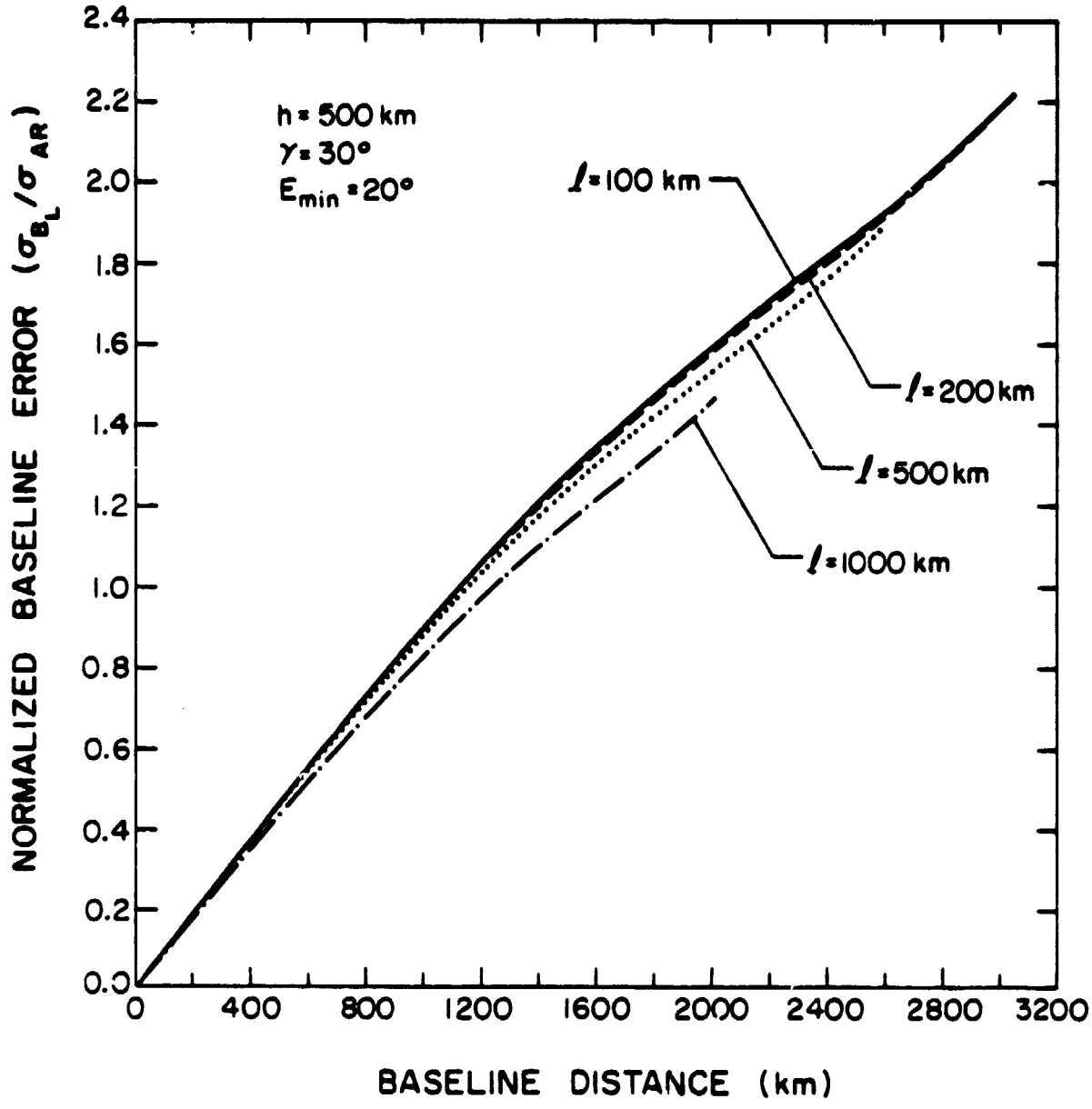

Figure 21. Normalized baseline error versus baseline for different satellite orbit separations in the correlated-path laser ranging system.

5. COORDINATE ERRORS FOR A SINGLE GROUND STATION

In this section, we examine the coordinate errors for a single station due to the effects of atmospheric refraction and see how they vary with respect to the orbital parameters. By referring to the coordinate covariance matrix of Equation (31), we see that the x-coordinate variance is zero, and the y- and z-coordinate variances of a single ground station are given by Equations (32) and (34), respectively. The geometry used to evaluate these two variances is almost the same as that described in Section 4 (Figure 4), with the exceptions that the baseline distance (B_L) between two stations is now replaced by the perpendicular distance between the x-axis and a ground station (y_D). This geometry is illustrated in Figure 22.

The formulas for the various elevation angles given by Equations (41) to (45) are still valid here with the term ($B_L \cos \gamma$) replaced by $2y_D$. By substituting these new equations into Equations (32), (34), (38) and (39), we can express the coordinate variances as

$$\sigma_y^2 = \frac{\sigma_\beta^2}{h^2 \ell^2} \left\{ C_1^2 \left[h^2 + \left(y_D + \frac{\ell}{2} \right)^2 \right]^2 - 2\rho C_1 C_2 \left[h^2 + \left(y_D - \frac{\ell}{2} \right)^2 \right] \left[h^2 + \left(y_D + \frac{\ell}{2} \right)^2 \right] \right.$$

$$\left. + C_2^2 \left[h^2 + \left(y_D - \frac{\ell}{2} \right)^2 \right]^2 \right\} \quad , \tag{59}$$

and

$$\sigma_z^2 = \frac{\sigma_\beta^2}{h^4 \ell^2} \left\{ C_1^2 \left[h^2 + \left(y_D + \frac{\ell}{2} \right)^2 \right]^2 \left(y_D - \frac{\ell}{2} \right)^2 - 2\rho C_1 C_2 \left[h^2 + \left(y_D - \frac{\ell}{2} \right)^2 \right] \right.$$

$$\left. \cdot \left[h^2 + \left(y_D + \frac{\ell}{2} \right)^2 \right] \left(y_D^2 - \frac{\ell}{4} \right)^2 + C_2^2 \left[h^2 + \left(y_D - \frac{\ell}{2} \right)^2 \right]^2 \left(y_D + \frac{\ell}{2} \right)^2 \right\} , \tag{60}$$

where

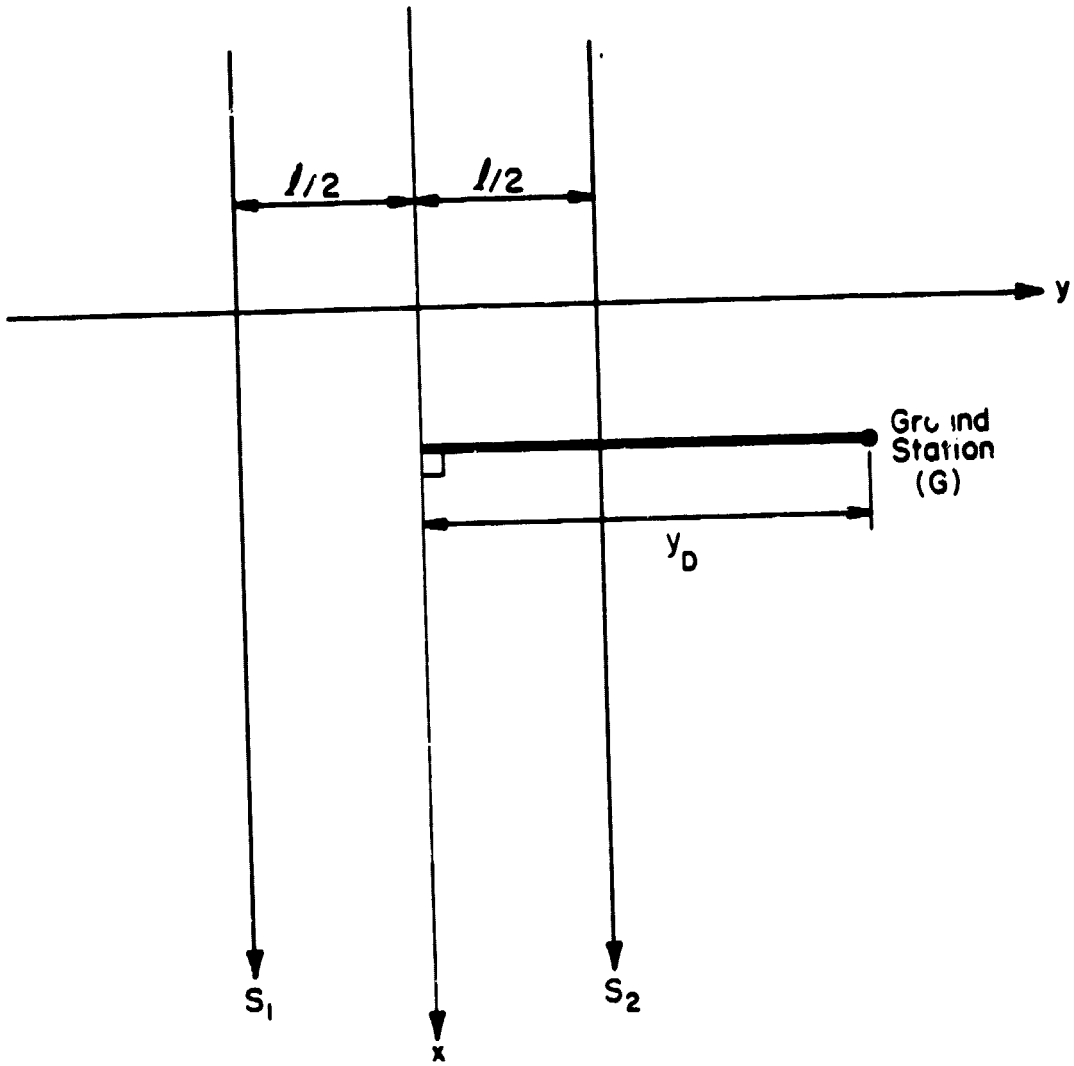

Figure 22. Ranging geometry for a single ground station.

$$1 < C_n = \frac{\frac{1}{4}\sin 2\phi_n + \frac{1}{2}\phi_n}{\frac{1}{32}\sin 4\phi_n + \frac{1}{4}\sin 2\phi_n + \frac{3}{8}\phi_n} < \frac{4}{3} \qquad n = 1,2, \tag{61}$$

$$\phi_n = \cos^{-1}\left(\frac{\sin E_n^0}{\sin E_n^M}\right) \qquad n = 1,2, \tag{62}$$

n denotes the nth satellite pass, and ρ is the β-error correlation coefficient associated with the measurements acquired by the ground station during the two passes.

By taking the square roots on both sides of Equations (59) and (60) and normalizing the results by the maximum atmospheric refraction error (σ_{AR}), we have the normalized rms coordinate errors

$$\frac{\sigma_y}{\sigma_{AR}} = \frac{\sin E_{min}}{h\ell}\left\{C_1^2\left[h^2 + \left(y_D + \frac{\ell}{2}\right)^2\right]^2 - 2\rho C_1 C_2\left[h^2 + \left(y_D - \frac{\ell}{2}\right)^2\right]\left[h^2 + \left(y_D + \frac{\ell}{2}\right)^2\right] + C_2^2\left[h^2 + \left(y_D - \frac{\ell}{2}\right)^2\right]^2\right\}^{1/2}, \tag{63}$$

and

$$\frac{\sigma_z}{\sigma_{AR}} = \frac{\sin E_{min}}{h^2\ell}\left\{C_1^2\left[h^2 + \left(y_D + \frac{\ell}{2}\right)^2\right]^2\left(y_D - \frac{\ell}{2}\right)^2 - 2\rho C_1 C_2\left[h^2 + \left(y_D - \frac{\ell}{2}\right)^2\right] \cdot \left[h^2 + \left(y_D + \frac{\ell}{2}\right)^2\right]\left(y_D^2 - \frac{\ell^2}{4}\right) + C_2^2\left[h^2 + \left(y_D - \frac{\ell}{2}\right)^2\right]^2\left(y_D + \frac{\ell}{2}\right)^2\right\}^{1/2}. \tag{64}$$

The approximate lower bounds for these coordinate errors can be found by assuming a zero y_D and letting C_n be unity. This yields

$$\frac{\sigma_y}{\sigma_{AR}} > \sin E_{min} (2 - 2\rho)^{1/2} \left(\frac{h}{\ell} + \frac{\ell}{4h} \right) , \tag{65}$$

and

$$\frac{\sigma_z}{\sigma_{AR}} > \frac{\sin E_{min}}{2} (2 + 2\rho)^{1/2} \left(1 + \frac{\ell^2}{4h^2} \right) . \tag{66}$$

By comparing Equation (63) with Equation (48), we can see that the characteristics of the y-coordinate error follow exactly the characteristics of the baseline error. This is to be expected because the y-coordinate error is the only error source contributing to the baseline error in the previous analysis. Equations (64) and (66) show that the z-coordinate error is directly related to the satellite orbit separation (ℓ) and is inversely related to the orbit altitude (h) for the small y_D. Furthermore, Equation (65) indicates that a zero y-coordinate error can only be obtained when the refraction errors during the two passes are positively correlated ($\rho = +1$); whereas, Equation (66) indicates that the negatively correlated refraction errors ($\rho = -1$) are necessary for the zero z-coordinate error. These results can be explained by the geometry of the ranging system. When y_D is zero, the satellite ground tracks are equidistant from each side of the ground station. If the refraction errors are positively correlated, this will give rise to the y-coordinate range errors of equal magnitudes and opposite directions on the two passes, and therefore, the resultant y-coordinate error for the station will be zero. Since both satellite orbits are above the station at equal altitudes, in order to have a zero z-coordinate error for the station (which means the z-coordinate range errors on the two passes are equal in magnitude but opposite in direction), the refraction errors during the two passes must be negatively correlated.

When y_D is large compared to ℓ, the coordinate errors can be approximated as

$$\frac{\sigma_y}{\sigma_{AR}} = \sin E_{min} \left(\frac{h}{\ell} + \frac{y_D^2}{h\ell} \right) (C_1^2 - 2\rho C_1 C_2 + C_2^2)^{1/2} \tag{67}$$

and

$$\frac{\sigma_z}{\sigma_{AR}} = \sin E_{min} \left(\frac{y_D}{\ell} + \frac{y_D^3}{h\ell} \right) (C_1^2 - 2\rho C_1 C_2 + C_2^2)^{1/2} \tag{68}$$

Equation (67) indicates that the y-coordinate error is proportional to the square of y_D. Whereas, Equation (68) indicates that the z-coordinate error is a linear and cubic functions of y_D. By comparing these two equations, we find that the z-coordinate error for a ground station can be a lot larger than the y-coordinate error if the satellite altitude (h) is small compared to y_D. When h and y_D are comparable, the coordinate errors of equal magnitudes are resulted. In this case, both coordinate errors are related directly to the satellite altitude (h) and inversely to the orbit separation (ℓ). It should also be noted that when y_D is large, C_1 and C_2 are approximately equal, and the minimum coordinate errors can be obtained when ρ equals unity. This means that the smallest possible station coordinate errors for large y_D can be achieved when the atmospheric refraction errors are positively correlated (this is analogous to the result obtained in Section 4 where the correlated-path ranging always gives the smallest baseline error).

6. CONCLUSION

Based upon the standard regression model and the geometry of the ranging sites, the general expression for the baseline error in the spherically symmetric atmosphere is derived.

It has been shown that the γ angle and, hence, the angle of intersection between the baseline and the satellite ground tracks play an important role in the baseline error determination. In particular, the minimum baseline error can be achieved when γ approaches 90°, that is, when the baseline of the two ground stations is parallel to the satellite ground tracks. Besides the fact that the baseline error has a strong dependence on the angle γ, the choices of minimum elevation angle, orbit altitude and orbit separation are also important in determining the magnitude of this error.

Figures (5) through (26) indicate that the baseline error grows rapidly as the baseline increases, and it can be more than an order of magnitude larger than the refraction error for the intercontinental baselines. In cases where the baselines are short, the baseline errors can be a fraction of the atmospheric refraction errors.

The analysis in this report does not consider the baseline error for the nonhomogeneous atmosphere. In the nonhomogeneous atmospheres, additional refraction error terms due to the gradient correction must be included. These terms may have a significant contribution to the total baseline error.

REFERENCES

[1] D. E. Smith, R. Kolenkiewicz, R. W. Agreen and P. J. Dunn, "Dynamic techniques for studies of secular variations in position from ranging to satellites," Proceedings of Symposium on the Earth's Gravitational Field and Secular Variations in Position, Sydney, Australia, November 1973.

[2] T. E. McGunigal, et al., "Satellite laser ranging work at the Goddard Space Flight Center," NASA Tech. Rep. X-723-75-172, July 1975.

[3] W. E. Hatch and D. C. Chin, "Erodyn program mathematical description version 7507," Automated Sciences Group, Inc., ASGI-TR-75-07, August 1975.

[4] D. E. Smith, R. Kolenkiewicz and P. J. Dunn, "Geodetic studies by laser ranging satellites," Geophysical Monograph Series Vol. 15, The Use of Artificial Satellites for Geodesy, Henriksen, Mancini and Chovitz, Ed., American Geophysical Union, 1972.

[5] C. S. Gardner, "Correction of laser tracking data for the effects of horizontal refractivity gradients," Appl. Opt., Vol. 16, September 1977.

[6] J. W. Marini and C. W. Murray, "Correction of laser ranging data for atmospheric refraction at elevations above 10 degrees," NASA Tech. Rep. X-159-73-351, November 1973.

[7] L. Mandel, "Phenomenological theory of laser beam fluctuations and beam mixing," Phys. Rev., 138 (3B), May 1965.

[8] J. B. Abshire, "A comparative study of optimum and suboptimum direct-detection laser ranging receivers," NASA Tech. Paper 1315, June 1978.

[9] C. G. Lehr, M. R. Pearlman, J. L. Scott, and J. Wohn, "Laser satellite ranging," Proceedings of Symposium on Laser Applications in the Geosciences, J. Gauger and F. F. Hall, Jr., Eds., Douglas Advanced Research Laboratories, June 1969.

[10] T. S. Englar, Jr., C. L. Hammond and B. P. Gibbs, "Covariance analysis of the airborne laser ranging system," Business and Technological System, Inc., BTS-TR-78-52, February 1978.

CUMULATIVE LIST OF RADIO RESEARCH LABORATORY REPORTS PREPARED UNDER NASA GRANT NSG-5049

RRL Rep. No. 469 - Gardner, C. S. (December 1975), The Effects of Random Path Fluctuations on the Accuracy of Laser Ranging Systems.

RRL Rep. No. 471 - Zanter, D. L., C. S. Gardner and N. N. Rao (January 1976), The Effects of Atmospheric Refraction on the Accuracy of Laser Ranging Systems.

RRL Rep. No. 477 - Gardner, C. S. and J. R. Rowlett (November 1976), Atmospheric Refraction Errors in Laser Ranging Data.

RRL Rep. No. 478 - Gardner, C. S. and B. E. Hendrickson (December 1976), Correction of Laser Ranging Data for the Effects of Horizontal Refractivity Gradients.

RRL Rep. No. 481 - Gardner, C. S. (January 1977), Statistics of the Residual Refraction Errors in Laser Ranging Data.

RRL Rep. No. 486 - Gardner, C. S. (June 1977), Comparison Between the Refraction Error Covariance Model and Ray Tracing.

RRL Rep. No. 488 - Gardner, C. S. (December 1977), Speckle Noise in Satellite Based Lidar Systems.

RRL Rep. No. 495 - Gardner, C. S. and G. S. Mercherle (April 1978), Speckle Noise in Direct-Detection Lidar Systems.

RRL Rep. No. 496 - Gardner, C. S. and A. M. Saleh (October 1978), Speckle Noise in Differential Absorption Lidar Systems.

RRL Rep. No. 499 - Gardner, C. S. (January 1979), A Technique for Remotely Measuring Surface Pressure from a Satellite Using a Multicolor Laser Ranging System.

RRL Rep. No. 502 - Palluch, E., J. Shelton and C. S. Gardner (May 1979), Operating Manual for the RRL 8 Channel Data Logger.

RRL Rep. No. 505 - Gardner, C. S. and R. Axford, Jr. (March 1980), Regression Models for Multicolor Satellite Laser Ranging.

RRL Rep. No. 510 - Gardner, C. S. (April 1981), Analysis of Target Signatures for Laser Altimeters.

RRL Rep. No. 514 - Tsai, B. and C. S. Gardner (December 1981), Remote Sensing of Sea State by Laser Altimeters.

RRL Rep. No. 519 - Im, K. E. and C. S. Gardner (September 1982), Atmospheric Refraction Effects on Baseline Error in Satellite Laser Ranging Systems.

PAPERS PUBLISHED

C. S. Gardner, "Effects of Random Path Fluctuations on the Accuracy of Laser Ranging Data," Applied Optics, 15, 2539-2545, October 1976.

C. S. Gardner, "Effects of Horizontal Refractivity Gradients on the Accuracy of Laser Ranging to Satellites," Radio Science, 11, 1037-1044, December 1976.

C. S. Gardner, "Correction of Laser Tracking Data for the Effects of Horizontal Refractivity Gradients," Applied Optics, 16, 2427-2432, September 1977.

C. S. Gardner, J. R. Rowlett, and B. E. Hendrickson, "Ray Tracing Evaluation of a Technique for Correcting the Refraction Errors in Satellite Tracking Data," Applied Optics, 17, 3143-3145, October 1978.

C. S. Gardner, "Technique for Remotely Measuring Surface Pressure from a Satellite Using a Multicolor Laser Ranging System," Applied Optics, 18, 3184-3189, September 15, 1979.

C. S. Gardner, "Target Signatures for Laser Altimeters: An Analysis," Applied Optics, 21, 448-453, February 1, 1982.

B. M. Tsai, and C. S. Gardner, "Remote Sensing of Sea State Using Laser Altimeters," Applied Optics, 21, November, 1982.